12 Kono Y, Mishina J, Yonemoto N, Kusuda S, Fujimura M: Neonatal correlates of adverse outcomes in very low-birthweight infants in the NICU network. Pediatr Int 2011;53:930–935.
13 Carlo WA, McDonald SA, Fanaroff AA, Vohr BR, Stoll BJ, Ehrenkranz RA, Andrews WW, Wallace D, Das A, Bell EF, Walsh MC, Laptook AR, Shankaran S, Poindexter BB, Hale EC, Newman NS, Davis AS, Schibler K, Kennedy KA, Sanchez PJ, Van Meurs KP, Goldberg RN, Watterberg KL, Faix RG, Frantz ID 3rd, Higgins RD: Association of antenatal corticosteroids with mortality and neurodevelopmental outcomes among infants born at 22 to 25 weeks' gestation. JAMA 2011;306:2348–2358.
14 Fowlie PW, Davis PG, McGuire W: Prophylactic intravenous indomethacin for preventing mortality and morbidity in preterm infants. Cochrane Database Syst Rev 2010;■■:CD000174.
15 Morgan J, Young L, McGuire W: Delayed introduction of progressive enteral feeds to prevent necrotising enterocolitis in very low birth weight infants. Cochrane Database Syst Rev 2011;■■:CD001970.
16 Sugiura T, Kouwaki M, Togawa Y, Sugimoto M, Togawa T, Koyama N: Neurodevelopmental outcomes at 18 months' corrected age of infants born at 22 weeks of gestation. Neonatology 2011;100:228–232.
17 Ishii N, Kono Y, Yonemoto N, Kusuda S, Fujimura M: Outcomes of infants born at 22 and 23 weeks' gestation. Pediatrics 2013;132:62–71.
18 Huttenlocher PR: Morphometric study of human cerebral cortex development. Neuropsychologia 1990;28:517–527.
19 Huttenlocher PR, Dabholkar AS: Regional differences in synaptogenesis in human cerebral cortex. J Comp Neurol 1997;387:167–178.
20 Shields A, Thomson M, Winter V, Coalson J, Rees S: Repeated courses of antenatal corticosteroids have adverse effects on aspects of brain development in naturally delivered baboon infants. Pediatr Res 2012;71:661–667.

The Journal of Immunology

Activation of an Innate Immune Receptor, Nod1, Accelerates Atherogenesis in *Apoe*$^{-/-}$ Mice

Shunsuke Kanno, Hisanori Nishio, Tamami Tanaka, Yoshitomo Motomura, Kenji Murata, Kenji Ihara, Mitsuho Onimaru, Sho Yamasaki, Hajime Kono, Katsuo Sueishi and Toshiro Hara

J Immunol 2015; 194:773-780; Prepublished online 8 December 2014;
doi: 10.4049/jimmunol.1302841
http://www.jimmunol.org/content/194/2/773

The Journal of Immunology is published twice each month by The American Association of Immunologists, Inc., 9650 Rockville Pike, Bethesda, MD 20814-3994.

Print ISSN: 0022-1767 Online ISSN: 1550-6606.

Activation of an Innate Immune Receptor, Nod1, Accelerates Atherogenesis in Apoe$^{2/2}$ Mice

Shunsuke Kanno,* Hisanori Nishio,*,† Tamami Tanaka,* Yoshitomo Motomura,‡ Kenji Murata,* Kenji Ihara,* Mitsuho Onimaru,x Sho Yamasaki,‡ Hajime Kono,{ Katsuo Sueishi,‖ and Toshiro Hara*

Atherosclerosis is essentially a vascular inflammatory process in the presence of an excess amount of lipid. We have recently reported that oral administration of a nucleotide-binding oligomerization domain (Nod)-1 ligand, FK565, induced vascular inflammation in vivo. No studies, however, have proven the association between Nod1 and atherosclerosis in vivo. To investigate a potential role of NOD1 in atherogenesis, we orally administered FK565 to apolipoprotein E knockout (Apoe$^{2/2}$) mice for 4 wk intermittently **and performed quantification of atherosclerotic lesions in aortic** roots and aortas, immunohistochemical analyses, and **microarray-based gene expression profiling of aortic roots. FK565 administration accelerated the development of atherosclerosis** in Apoe$^{2/2}$ mice, and the effect was dependent on Nod1 in non–bone marrow origin cells by bone marrow transplantation experiments. Immunohistochemical studies revealed the increases in the accumulation of macrophages and CD3 T cells within the plaques in aortic roots. Gene expression analyses of aortic roots demonstrated a marked upregulation of the Ccl5 gene during **early stage of atherogenesis, and the treatment with Ccl5 antagonist significantly inhibited the acceleration of atherosclerosis in** FK565-administered Apoe$^{2/2}$ mice. Additionally, as compared with Apoe$^{2/2}$ mice, Apoe and Nod1 double-knockout mice showed **reduced development of atherosclerotic lesions from the early stage as well as their delayed progression and a significant reduction** in Ccl5 mRNA levels at 9 wk of age. Data in the present study show that the Nod1 signaling pathway in non–bone marrow-derived cells contributes to the development of atherosclerosis. The Journal of Immunology, 2015, 194: 773–780.

Atherosclerosis is a chronic inflammatory disease of vessel walls, characterized by the accumulation of leukocytes and their subsequent differentiation into cholesterol-laden foam cells (1). Innate and acquired immune systems are considered to be associated with the development of atherosclerosis (2–4). Concerning the innate immunity, epidemiological studies and animal experiments showed that infectious agents and their components contribute to the local chronic inflammatory process underlying atherosclerosis (4–7). The innate immune receptors recognize structurally conserved moieties and work as pattern recognition receptors (PRRs) such as TLRs, nucleotide oligomerization domain–like receptors (NLRs), retinoic acid–inducible gene-I-like receptors or C-type lectin receptors (8). Among PRR families, there is a line of evidence that TLRs, especially TLR4, TLR2, and their signaling molecule, MyD88 (7, 9, 10), play important roles in the development of atherosclerosis by initiating an inflammatory response to several pathogenic bacteria such as Chlamydophila pneumoniae or Porphyromonas gingivalis (5, 6).

With respect to NLRs, only a limited number of studies have shown that NLRs might be involved in atherosclerosis (11, 12). More than 20 NLRs have been identified in humans (8). Nucleotide-binding oligomerization domain (NOD)-1 is an intracellular sensor of bacterial peptidoglycan (PGN), and it is constitutively expressed in many types of cells, including endothelial cells (13, 14). NOD1 specifically recognizes a diaminopimelic acid–containing dipeptide, derived mostly from bacteria (13), and activates the signal pathway via the transcription factor NF-kB (14, 15). Recently, pure synthetic ligands for NLRs, such as FK156 and FK565 for NOD1 or MDP for NOD2, have been available for studies on the biological significance of these receptors. We have recently reported that oral administration of a synthetic Nod1 ligand FK565 efficiently induced acute vasculitis in mice (16). Therefore, it would make sense to investigate the contribution of a long-term exposure of a small dose of NOD1 ligand to the development of atherosclerosis, a chronic vascular inflammatory disease.

In this study, we show that oral administration of FK565 accelerated the development of atherosclerosis in apolipoprotein E knockout (Apoe$^{2/2}$) mice, and the effect was dependent on Nod1 in non–bone marrow-derived cells by transplantation experiments. By microarray analysis, we found that Ccl5 expression was sig-

*Department of Pediatrics, Graduate School of Medical Sciences, Kyushu University, Fukuoka 812-8582, Japan; †Center for the Study of Global Infection, Kyushu University Hospital, Fukuoka 812-8582, Japan; ‡Division of Molecular Immunology, Medical Institute of Bioregulation, Kyushu University 812-8582, Fukuoka, Japan; xDivision of Pathophysiological and Experimental Pathology, Department of Pathology, Kyushu University, Fukuoka 812-8582, Japan; {Department of Internal Medicine, Teikyo University School of Medicine, Tokyo 173-8605, Japan; and ‖Department of Research and Education, National Hospital Organization Fukuoka–Higashi Medical Center, Fukuoka 811-3195, Japan

Received for publication October 21, 2013. Accepted for publication November 13, 2014.

This work was supported by grants from the Japan Society for the Promotion of Science and Health and Labour Sciences Research Grants from the Ministry of Health, Labor and Welfare, Japan.

The microarray data presented in this article have been submitted to the Gene Expression Omnibus (http://www.ncbi.nlm.nih.gov/geo/) under accession number GSE48947.

Address correspondence and reprint requests to Dr. Shunsuke Kanno, Department of Pediatrics, Graduate School of Medical Sciences, Kyushu University, 3-1-1 Maidashi, Higashi-ku, Fukuoka, 812-8582, Japan. E-mail address: kannos@pediatr.med.kyushu-u.ac.jp

The online version of this article contains supplemental material.

Abbreviations used in this article: Apoe, apolipoprotein E; EVG, Elastica–van Gieson; NLR, nucleotide oligomerization domain–like receptor; NOD, nucleotide-binding oligomerization domain; PGN, peptidoglycan; PRR, pattern recognition receptor; RIP2, receptor-interacting protein 2; a-SMA, a–smooth muscle actin.

www.jimmunol.org/cgi/doi/10.4049/jimmunol.1302841

nificantly upregulated by FK565 administration in aortic roots during early stage of atherogenesis, and the treatment with Ccl5 antagonist significantly inhibited the acceleration of atherosclerosis in FK565-administered Apoe$^{-/-}$ mice. Finally, we demonstrated that Nod1 deficiency resulted in reduced development of atherosclerotic lesions as well as their delayed progression in Apoe$^{-/-}$ mice, indicating the contribution of Nod1 ligand to the development of atherosclerosis.

Materials and Methods

Animals and bone marrow transplantation

C57BL/6J Apoe$^{-/-}$ mice were purchased from The Jackson Laboratory. Nod1$^{-/-}$ mice in the C57BL/6 background were a gift from Tak Mak, University Health Network. Nod1$^{-/-}$ mice were crossed with Apoe$^{-/-}$ C57BL/6 mice. Heterozygous mice were intercrossed to generate homozygous Apoe$^{-/-}$ mice bearing combinations of Nod1$^{+/+}$ and Nod1$^{-/-}$ mice. The genotype for Apoe or Nod1 was confirmed using primers and conditions described in the The Jackson Laboratory Web site or the previous report (17), respectively. All mice were fed a normal chow diet and housed in a specific pathogen-free environment throughout the experiment. Drinking water and food for mice did not contain Nod1-stimulatory activity by a bioassay using HEK-Blue murine NOD1 cells (InvivoGen, San Diego, CA), which were HEK293 cells carrying a NF-kB reporter and transfected with a Nod1 construct. The study protocol was reviewed and approved by the Animal Care and Treatment Committee of Kyushu University.

For bone marrow transplantation studies, 9-wk-old male Apoe$^{-/-}$ Nod1$^{-/-}$ mice and Apoe$^{-/-}$ Nod1$^{+/+}$ mice received 8 Gy total body irradiation to eliminate endogenous bone marrow stem cells and most of the bone marrow–derived cells, including macrophages. Bone marrow cells for transplantation into the irradiated mice were prepared by flushing both femurs of male Apoe$^{-/-}$ Nod1$^{-/-}$ or Apoe$^{-/-}$ Nod1$^{+/+}$ mice. Donor cells were washed, suspended in sterile RPMI 1640 medium with 2% FCS, and concentrated to 1 3 10^8 cells/ml. Three hours after irradiation, 1 3 10^7 bone marrow cells were injected into the tail vein of a mouse. Successful reconstitution was confirmed by PCR genotyping of recipient mouse peripheral blood cells.

FK565 administration and Met-RANTES treatment

FK565, a synthetic and pure Nod1 ligand, was supplied by Astellas Pharma (Tokyo, Japan). At 5 wk of age, mice were randomized to FK565-administered and nonadministered groups. The administration protocol was as follows: two doses of FK565 solution (10 or 50 mg), reconstituted at 10 mg/ml in sterile distilled H_2O, was orally administered once a day for 2 consecutive days and then observed for the following 5 d per week. This course of the intermittent administration was continued for 4 wk, and mice were euthanized 6 d after the last administration. For the transplanted mice, FK565 was administered for four courses from 7 wk after bone marrow transplantation and euthanized at 20 wk of age. After euthanasia, serum was obtained from the vena cava after an overnight fast.

Because the Ccl5 antagonist Met-RANTES has been used in vivo in animal models of atherosclerosis, we determined the protocol of Met-RANTES treatment according to previous reports (18–20) with minor modifications. Met-RANTES (R&D Systems, Minneapolis, MN) was administered i.p. in a single dose of 50 mg diluted in PBS 30 min before FK565 administration. In parallel, control mice received a similar volume of sterile PBS.

Antibiotic treatment protocol

Mice were treated with 1 g/l ampicillin (Wako Pure Chemicals, Osaka, Japan) dissolved in drinking water, as well as an antibiotic concoction consisting of 5 mg/ml vancomycin, 10 mg/ml neomycin, and 10 mg/ml metronidazole (all from Wako Pure Chemicals) by oral gavage every 24 h according to the method as described (21). Gavage volume of 20 ml/kg body weight was delivered with a polytetrafluoroethylene tube with prior sedation of the mice. The antibiotic administration was initiated at 5 wk of age and continued for 5 wk from 1 wk before 4 wk FK565 administration.

Intestinal depletion was assessed by collecting feces, homogenizing in 1 ml sterile PBS, and serially diluting and plating on trypticase soy agar with 5% sheep blood (BD Biosciences, Franklin Lakes, NJ) for 48 h at 37°C aerobically or in an anaerobic chamber (AnaeroPack system; Mitsubishi Gas Chemical, Tokyo, Japan). The number of bacteria per milligram of feces was calculated based on the CFU counted in each serial dilution.

Histological and immunohistological analyses of aortic roots

After mice were euthanized, the hearts were removed rapidly after perfusion with PBS. The hearts were embedded in optimal cutting temperature compound (Sakura Finetek Japan, Tokyo, Japan) and quickly frozen in liquid nitrogen or 4% paraformaldehyde-fixed and paraffin-embedded for histological and immunohistological analyses. Sixty serial cross-sections (6 mm thick) of the aortic root were prepared from the site where the three aortic valves first appeared according to the method as described (22). The atherosclerotic lesions in the aortic root were investigated at six locations, each separated by 60 mm. Three serial frozen sections prepared from each location were conventionally stained with Sudan IV (Tokyo Kasei Kogyo, Tokyo, Japan), Elastica–van Gieson (EVG), and H&E stains. Similarly, seven serial paraffin-embedded sections prepared from each location were stained with H&E, EVG, MOMA-2 (macrophage)–specific Ab (1:100; AbD Serotec, Raleigh, NC), CD3 (T cell)–specific Ab (1:500; Abcam, Cambridge, U.K.), NIMP-R14 (neutrophil)–specific Ab (1:500; Abcam), a–smooth muscle actin (a-SMA)–specific Ab (1:100; Dako, Glostrup, Denmark), and Ccl5-specific Ab (1:10; R&D Systems). As a negative control, nonimmune IgG or isotype control was used. Detection and visualization of primary Ab binding was done as described (16). For quantitative estimation of the plaque contents, we analyzed absolute areas or numbers of cells staining positive for a respective marker within the plaque area by using Adobe Photoshop CS5 and National Institutes of Health ImageJ software. The average value for the six locations for each animal was used for analysis.

Assessment of atherosclerosis in aortas

Immediately after mice were euthanized, the aorta was dissected from the proximal ascending aorta to the bifurcation of the iliac artery. The adventitial tissue was carefully removed, and then the aorta was opened longitudinally, fixed in 10% buffered formalin overnight, stained with Sudan IV, pinned on a black wax surface, and photographed for quantification of en face plaque areas. En face images were obtained by a stereomicroscope (SteREO Lumar V12; Carl Zeiss, Oberkochen, Germany) equipped with a digital camera (AxioCam MRc5; Carl Zeiss) and analyzed by Adobe Photoshop CS5 and National Institutes of Health ImageJ software. Lipid lesion formation was analyzed by the determination of the percentage area stained with Sudan IV to the total aortic area. Quantification of atherosclerotic lesions was performed by a single observer blinded to the experimental protocol.

Microarray analysis

To obtain sufficient amount of RNA for microarray analysis, the aortic roots removed from three animals were mixed, homogenized, and used as one sample. Two independent experiments were performed. Total RNA was extracted with an RNeasy fibrous tissue kit (Qiagen, Hilden, Germany) and amplified using an amino allyl MessageAmp II aRNA amplification kit (Ambion, Austin, TX). Double-stranded cDNA was synthesized from total RNA using oligo(dT) primer with a T7 RNA polymerase promoter site added to the 39-end. Then, in vitro transcription was performed in the presence of amino allyl uridine-59-triphosphate to produce multiple copies of amino allyl-labeled cRNA. Amino allyl–labeled cRNA was purified, reacted with N-hydroxy succinimide esters of Cy3 (GE Healthcare, Little Chalfont, U.K.) using NimbleGen's protocol and hybridized for 19 h at 42°C to the Mouse Gene Expression 12 3 135K array (100718_MM9_EXP_HX12; Roche NimbleGen, Madison, WI) consisting of 44,170 genes. The arrays were scanned on GenePix 4000B (Molecular Devices, Sunnyvale, CA). The averages of triplicate spot intensities were extracted using NimbleScan v2.5 (Roche NimbleGen) and processed using robust multiarray analysis method (16). The scaled gene expression values were imported into GeneSpring 11.5.1 software (Agilent Technologies, Santa Clara, CA) for preprocessing and data analysis (16). The expression value of each gene was normalized to the 75th percentile shift expression of all genes. Probe sets were deleted from subsequent analysis when they were displayed an absolute value , 30 in all experiments. The fold change was calculated as the ratio of the two group means based on the observed signal values. Microarray data were deposited in Gene Expression Omnibus (http://www.ncbi.nlm.nih.gov/geo/) under accession no. GSE48947.

Quantitative real-time RT-PCR

Total RNA was extracted from the aortic root using RNeasy fibrous tissue, followed by cDNA synthesis using a high-capacity RNA-to-cDNA kit (Applied Biosystems, Foster City, CA). Mouse Ccl5, Cxcl16, Ccl8, and Gapdh expression levels were analyzed by TaqMan gene expression assays Mm01302427_m1, Mm00469712_m1, Mm01297183_m1, and Mm-99999915_g1 (Applied Biosystems), consisting of a 203 mix of unlabeled PCR primers and a TaqMan MGB probe (FAM dye-labeled), and TaqMan gene expression master mix (Applied Biosystems). Mouse Gapdh was used as internal controls. These TaqMan probes were labeled with the quencher TAMRA (emission I, 582 nm) at the 39-end through a linker-arm nucleotide. The mRNA expression levels of the targeted genes were quantified by the StepOne real-time PCR system and the StepOne software

v2.1 (Applied Biosystems). To calculate the relative expression level, the level of gene expression was divided by that of Gapdh. All experiments were carried out in duplicate and repeated three times for confirmation.

Serum lipid, glucose, and insulin analyses

Total cholesterol and triglyceride concentrations in the murine sera were measured with a LabAssay cholesterol kit and a LabAssay triglyceride kit (Wako Pure Chemicals), respectively. Blood glucose levels were determined with a Medisafe-Mini glucose meter (Terumo, Tokyo, Japan). Serum insulin levels were measured with a mouse insulin ELISA kit (Mercodia, Uppsala, Sweden). The homeostasis model assessment of insulin resistance index ([glucose (mg/dl) 3 insulin (mU/ml)]/405) was calculated.

Statistical analysis

Data were analyzed by Student t test, Dunnett test, or Tukey–Kramer honestly significant difference test using JMP version 8.0 (SAS Institute, Cary, NC). Values of p , 0.05 were considered statistically significant.

Results

Activation of Nod1 by the orally administered agonist accelerates atherogenesis in Apoe$^{2/2}$ mice

To investigate the effect of a Nod1 ligand on atherosclerosis, we orally administered FK565, a pure synthetic Nod1 ligand, to Apoe$^{2/2}$ male mice fed a chow diet. After preliminary experiments with orally administered FK565 at different doses consecutively or intermittently in Apoe$^{2/2}$ mice (data not shown), we analyzed the effect of orally administered FK565 on 9-wk-old Apoe$^{2/2}$ mice at 10 or 50 mg twice a week for 4 wk from 5 wk of age (Fig. 1A). No significant differences between the body weight and serum cholesterol and triglyceride levels of both groups of mice were observed (Supplemental Table I). Compared with the nonadministered group, a dose-dependent effect of FK565 was observed in the development of atherosclerosis in aortic roots with the lesion volumes of 1.85-fold (85%) increase at 10 mg and 5.49-fold (449%) increase at 50 mg FK565 in the FK565-administered group (Fig. 1B, 1D). In the FK565-administered group, a similar effect was also observed on the plaque formation in aortas of 1.10-fold (10%) increase at 10 mg and 33.9-fold (3289%) increase at 50 mg FK565 (Fig. 1C, 1E). To confirm the specificity of the FK565 treatment for Nod1, we studied Apoe$^{2/2}$ Nod1$^{2/2}$ mice in the same manner. There were no differences in the body weight and serum cholesterol or triglyceride levels in both groups of mice (Supplemental Table I). The plaque formation results showed no significant differences between FK565-administered Apoe$^{2/2}$ Nod1$^{2/2}$ mice and nonadministered mice (Fig. 1D, 1E). These results clearly demonstrated that oral administration of a pure synthetic Nod1 ligand accelerated the development of atherosclerosis in Apoe$^{2/2}$ mice in a Nod1-dependent manner.

To rule out the possibility that oral administration of FK565 alters the composition of gut commensal bacteria and the dysbiosis induces acceleration of atherosclerosis, we depleted the intestinal microbiota by providing antibiotics in drinking water and with oral gavage of the antibiotic concoction according to the previous report (21). Even in gut flora–depleted mice, FK565 administration accelerated the development of atherosclerosis, suggesting that the acceleration of atherosclerosis by orally administered FK565 does not depend on alteration of the composition of gut commensal bacteria (Supplemental Fig. 1).

Immunohistochemical studies of atherosclerotic lesions by a Nod1 ligand

To explore the effects of Nod1 ligand on the formation of atherosclerotic lesions, we performed immunohistochemical studies of vessel-wall constituents within the plaques in aortic roots. FK565-administered Apoe$^{2/2}$ mice showed a significantly higher level of macrophage and T cell infiltration within the plaques than did nonadministered Apoe$^{2/2}$ mice. Neutrophil numbers within the plaques in FK565-administered Apoe$^{2/2}$ mice also showed an

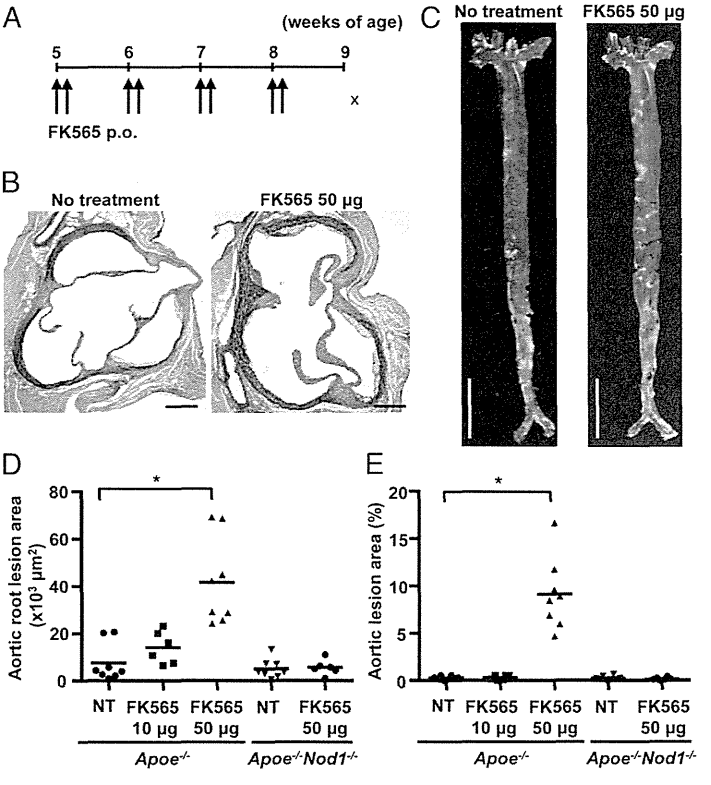

FIGURE 1. Acceleration of atherosclerosis by oral administration of FK565 in Apoe$^{2/2}$ mice. (A) Protocol for intermittent administration of FK565 (10 or 50 mg once a day, 2 d/wk, 4 wk) as described in Materials and Methods. p.o., per os. (B and C) Representative aortic roots (B) stained with EVG and aortas (C) stained with Sudan IV in Apoe$^{2/2}$ mice with or without FK565 administration at 9 wk of age. Scale bars, 200 mm (B) and 500 mm (C). (D and E) Quantification of atherosclerotic lesion areas of aortic roots (D) and aortas (E) in Apoe$^{2/2}$ mice with or without FK565 administration at 9 wk of age. Bars represent means (n = 6–8/group). *p , 0.01 versus nonadministered mice with each genotype (Dunnett test). NT, no treatment.

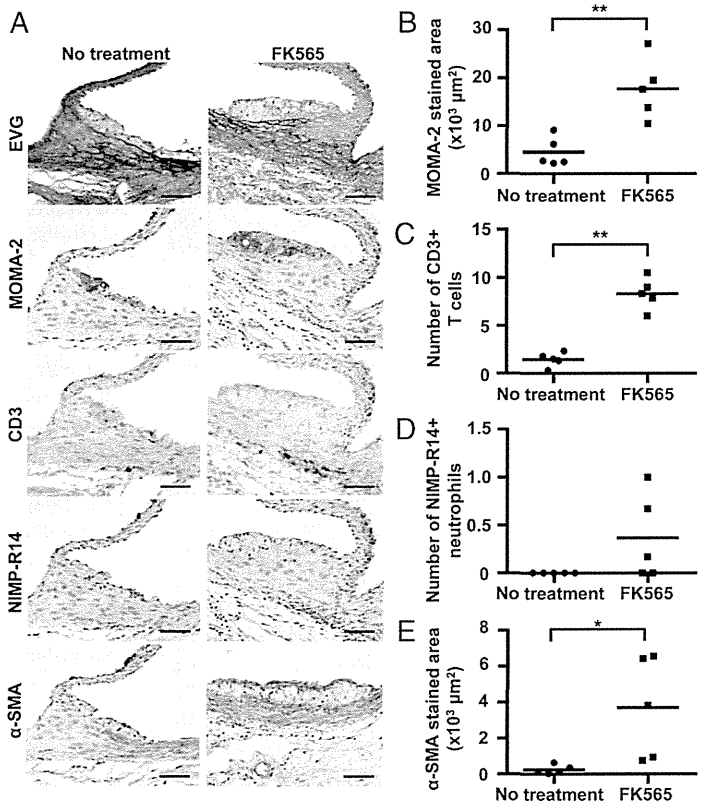

FIGURE 2. Immunohistochemical studies of atherosclerotic lesions by oral administration of FK565. (A) Representative aortic roots stained with EVG, MOMA-2, CD3, NIMP-R14, and a-SMA in Apoe$^{-/-}$ mice with or without FK565 administration at 9 wk of age. Scale bars, 50 mm. (B–E) Quantification of areas or numbers of cells positively stained for MOMA-2, CD3, NIMP-R14, and a-SMA within plaques in Apoe$^{-/-}$ mice with or without FK565 administration at 9 wk of age. Bars represent means (n = 5/group). *p , 0.05, **p , 0.01 (Student t test).

increasing tendency than did those in nonadministered Apoe$^{-/-}$ mice, although statistically not significant (Fig. 2A–D).

The previous report demonstrated that smooth muscle cells were intermingled with foam cells or tended to form a cap at the top of lesion in Apoe$^{-/-}$ mice at 10–15 wk of age (23). A marked increase of smooth muscle cell content in the plaques was observed in the FK565-administered group (p = 0.026; Fig. 2A, 2E). These results suggested that Nod1 ligand accelerated the progression of advanced atherosclerotic lesions, with a remarkable increase of macrophage and T cell infiltration in the plaque.

Contribution of Nod1 in nonhematopoietic cells to the increased atherogenesis by Nod1 ligand administration

As mentioned above, the effect of FK565 in atherogenesis was solely mediated by Nod1. Accordingly, to further test whether non–bone marrow-derived cells expressing Nod1 would contribute to the development of atherosclerosis by FK565 administration, we performed bone marrow transplantation experiments at 20 wk of age. All mice received FK565 for four courses. As expected, the atherosclerotic lesions in aortic roots of Apoe$^{-/-}$ mice with Apoe$^{-/-}$ bone marrow cells were significantly larger than those of Apoe$^{-/-}$ Nod1$^{-/-}$ mice transplanted with Apoe$^{-/-}$ Nod1$^{-/-}$ bone marrow (Fig. 3). Similarly, in chimeric Apoe$^{-/-}$ mice with Apoe$^{-/-}$ Nod1$^{-/-}$ bone marrow cells, the atherosclerotic lesions were significantly larger than those of Apoe$^{-/-}$ Nod1$^{-/-}$ mice transplanted with either Apoe$^{-/-}$ or Apoe$^{-/-}$ Nod1$^{-/-}$ bone marrow. Conversely, chimeric Apoe$^{-/-}$ Nod1$^{-/-}$ mice with Apoe$^{-/-}$ bone marrow cells had significantly smaller atherosclerotic lesions than did Apoe$^{-/-}$ mice transplanted with either Apoe$^{-/-}$ or Apoe$^{-/-}$ Nod1$^{-/-}$ bone marrow (Fig. 3). The data for total aortic plaque formation showed the same trends as did the data for aortic root lesion area discussed above (data not shown). These results indicated that non–bone marrow-derived cells had a pivotal role in acceleration of atherosclerosis induced by Nod1.

Ccl5 is a key chemokine in atherogenesis induced by orally administered Nod1 agonist

To explore the mechanisms underlying the progression of atherosclerosis provoked by Nod1 ligand stimulation, we performed microarray gene expression profiling of the aortic roots of 9-wk-old Apoe$^{-/-}$ mice with or without four courses of FK565 administration. Comparative analysis revealed that 1777 genes were up-

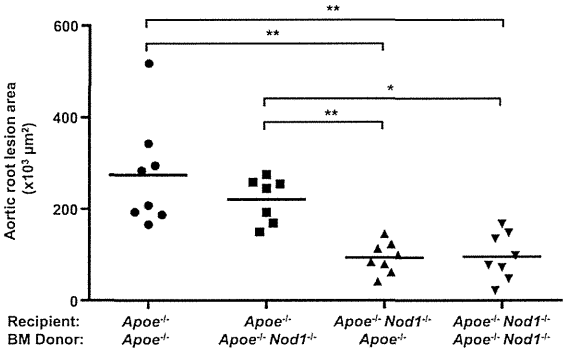

FIGURE 3. Acceleration of atherosclerosis by FK565 depends on Nod1 in nonhematopoietic cells. Quantification of atherosclerotic lesion areas of aortic roots in Apoe$^{-/-}$ and Apoe$^{-/-}$ Nod1$^{-/-}$ 20-wk-old mice underwent bone marrow (BM) reconstitution with BM from Apoe$^{-/-}$ or Apoe$^{-/-}$ Nod1$^{-/-}$ donors. All mice were orally administered FK565 (50 mg once a day, 2 d/wk) from 16 to 19 wk of age and fed a chow diet. Bars represent means (n = 7–8/group). *p , 0.05, **p , 0.01 (Tukey–Kramer honestly significant difference test).

regulated in the aortic roots of FK565-administered mice compared with those of nonadministered mice (Fig. 4A). We also analyzed gene expression in 6-wk-old Apoe$^{-/-}$ mice after only one course of FK565 administration, when there was weak accumulation of macrophages in the lesions, which was recognized as the initial stage of atherosclerosis (23) (data not shown). The analysis revealed that 1401 genes were upregulated by one course of FK565 administration, and 100 genes were consistently upregulated by FK565 administration in both time points, indicating that the 100 genes contributed to the initial and early stages of atherosclerosis induced by Nod1 agonist. A gene ontology analysis of the 100 genes showed that a number of biological process terms were associated with immune response (Supplemental Table II). Therefore, we focused on chemokine/cytokine genes. As expected, we identified a number of chemokine/cytokine genes known to be linked to atherosclerosis. The genes upregulated by FK565 in 6-wk-old Apoe$^{-/-}$ mice included Ccl4, Ccl5, Ccl8, Cxcl16, and Il2rb, which are involved in recruitment and activation of macrophage and lymphocyte. In contrast, in 9-wk-old Apoe$^{-/-}$ mice, genes associated with recruitment and activation of inflammatory cells, including chemokine/chemokine receptor genes (Cx3cl1, Ccl3, Ccl5, Ccl8, Cxcl1, Cxcl12, Cxcl16, Ccr2, Ccr5, Cxcr3, and Cxcr6) and IL genes (Il1b and Il6) were upregulated. In both time points, we observed that three genes were elevated . 2-fold (Fig. 4B). To validate the microarray data, we compared expression levels by real-time RT-PCR of these three genes in Apoe$^{-/-}$ mice with or without FK565 administration after both one and four courses and found that only one gene, Ccl5, also known as RANTES, was significantly upregulated by FK565 administration at both time points (Fig. 4C). Immunore-

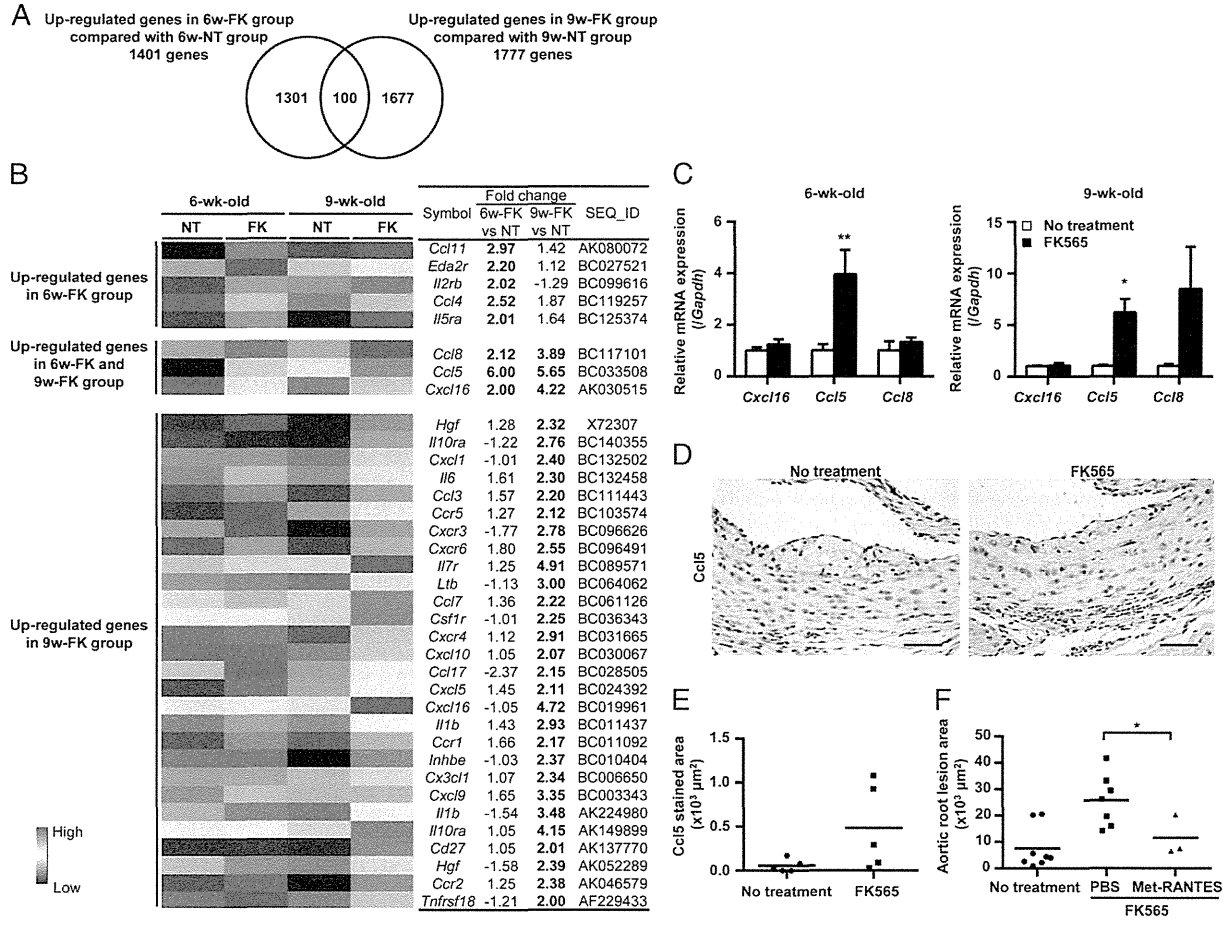

FIGURE 4. Effect of Ccl5 on atherogenesis induced by oral administration of FK565. In microarray analysis (A and B), total RNA extracted from the aortic roots in Apoe$^{-/-}$ mice with or without FK565 administration (FK and NT, respectively) at the age of 6 and 9 wk (6w and 9w, respectively) is shown. Each experiment sample contained three aortic roots from three mice, and two experiments were performed in each group. (A) Venn diagram of upregulated genes in the aortic roots of FK565-administered mice at 6 and/or 9 wk of age. (B) Gene expression ratio and heat map analysis of cytokine/chemokine genes expressed 2-fold higher in FK565-administered Apoe$^{-/-}$ mice than in nonadministered Apoe$^{-/-}$ mice at 6 or 9 wk of age. Each column represents the mean of the expression levels in each group of replicates. As shown on the color bar, red and blue indicate high and low expressions, respectively. Gene symbols, fold changes in each comparison, and GenBank accession numbers are presented in the right columns. Fold changes in bold refer to upregulation . 2-fold in each comparison. Data were deposited in Gene Expression Omnibus (http://www.ncbi.nlm.nih.gov/geo/) under accession number GSE48947. (C) RT-PCR analysis of Cxcl16, Ccl5, and Ccl8 genes in aortic roots of Apoe$^{-/-}$ mice with or without FK565 administration at the age of 6 and 9 wk. Gene expression was normalized to expression of Gapdh. Relative expression levels to the values observed in aortic root from nonadministered Apoe$^{-/-}$ mice are presented as mean 6 SEM (n = 5/group). (D and E) Representative microphotographs (D) and the quantification (E) of positive-stained areas for Ccl5 in aortic roots of Apoe$^{-/-}$ mice with or without FK565 administration at 9 wk of age. Scale bars, 50 mm (D). Bars represent means (n = 5/group) (E). (F) Quantitative comparison of atherosclerotic lesion areas of aortic roots in FK565-administered Apoe$^{-/-}$ mice with i.p. injection of PBS or Met-RANTES before every FK565 administration. Data of nonadministered Apoe$^{-/-}$ mice are presented as a control. Bars represent means (n = 3–8/group). *p , 0.05, **p , 0.01 (Student t test).

activity for Ccl5 was localized in the intimal areas (Fig. 4D), and Nod1 ligands slightly increased Ccl5 levels in the lesions of Apoe$^{-/-}$ mice, but without a statistically significant difference (Fig. 4E). To determine a role of Ccl5 in the atherosclerosis progression exerted by Nod1 activation, we investigated whether injection of a Ccl5 antagonist, Met-RANTES, could inhibit the acceleration of atherosclerosis in FK565-administered Apoe$^{-/-}$ mice. As expected, Met-RANTES–treated mice showed a significant decrease of atherosclerotic lesion area in aortic root, compared with PBS-treated mice (Fig. 4F), and they had a similar volume of plaques in aortic roots of Apoe$^{-/-}$ mice without FK565 administration. These results suggested that Ccl5 plays a crucial role in the acceleration of atherosclerosis induced by FK565.

To determine which cell type frequencies, macrophages or T cells, were altered after Met-RANTES administration, we performed immunohistochemical studies in aortic roots of FK565-administered mice with or without Met-RANTES administration. Both MOMA-2$^+$ macrophages and CD3$^+$ T cells in atherosclerotic lesions significantly decreased after Met-RANTES administration, suggesting that Ccl5 contributes to accumulation of both cell types in the atherosclerotic lesions (Supplemental Fig. 2A, 2B).

Nod1 deficiency reduces atherosclerotic lesion and Ccl5 gene expression in aortic roots

To determine whether Nod1 signaling pathway contributes to the early step of atherosclerosis, we studied Apoe$^{-/-}$ and Apoe$^{-/-}$ Nod1$^{-/-}$ male mice at the ages of 9, 12, 20, and 40 wk. Apoe$^{-/-}$ Nod1$^{-/-}$ mice showed modest elevations of serum cholesterol and triglyceride levels compared with those in Apoe$^{-/-}$ mice, but there were no significant differences (Supplemental Table I). Additionally, no difference was observed in the fasting blood glucose levels, serum insulin levels, or homeostasis model assessment of insulin resistance values between Apoe$^{-/-}$ and Apoe$^{-/-}$ Nod1$^{-/-}$ mice at 20 wk of age (data not shown). Nonetheless, Apoe$^{-/-}$ Nod1$^{-/-}$ mice showed 43, 63, and 26% decreases of atherosclerotic lesion areas in aortic root, compared with those in their age-matched Apoe$^{-/-}$ mice, at the ages of 12, 20, and 40 wk, respectively (Fig. 5A, 5C). By analysis of aortic lesion areas, Apoe$^{-/-}$ and Apoe$^{-/-}$ Nod1$^{-/-}$ mice had plaques from 20 wk of age, and they had similar distribution patterns of plaques, with the highest density occurring in the lesser curvature of the aortic arch at 40 wk of age (Fig. 5B). However, plaque formation areas in aortas were significantly reduced (54 and 25%) by Nod1 deficiency at the age of 20 and 40 wk, respectively (Fig. 5B, 5D). These results demonstrated that Nod1 deficiency not only attenuated early atherogenesis but also decelerated the progression of atherosclerosis.

To determine the cellular mechanism for the decelerated atherogenesis by Nod1 deficiency, we analyzed the cell composition of atherosclerotic lesions of Apoe$^{-/-}$ mice and Apoe$^{-/-}$ Nod1$^{-/-}$ mice by immunohistochemical studies. The areas for MOMA-2$^+$ macrophages or a-SMA$^+$ smooth muscle cells as well as the numbers of CD3$^+$ T cells or NIMP-R14$^+$ neutrophils in atherosclerotic lesions of Apoe$^{-/-}$ Nod1$^{-/-}$ mice were smaller than those in Apoe$^{-/-}$ mice, but the differences were not statistically significant (Supplemental Fig. 2C–F).

In microarray and RT-PCR analyses, Nod1 ligands increased Ccl5 mRNA levels in aortic root of Apoe$^{-/-}$ mice compared with nonadministered mice (Fig. 4B, 4C). Ccl5 was predominantly upregulated in early plaques (24) and is considered to be important in early lesion formation. Therefore, we examined Ccl5 gene expression levels in aortic root of Apoe$^{-/-}$ and Apoe$^{-/-}$ Nod1$^{-/-}$ mice in early stages of atherosclerosis at 6, 9, 12, and 20 wk of age. At 6–12 wk of age, Ccl5 mRNA levels in aortic roots of

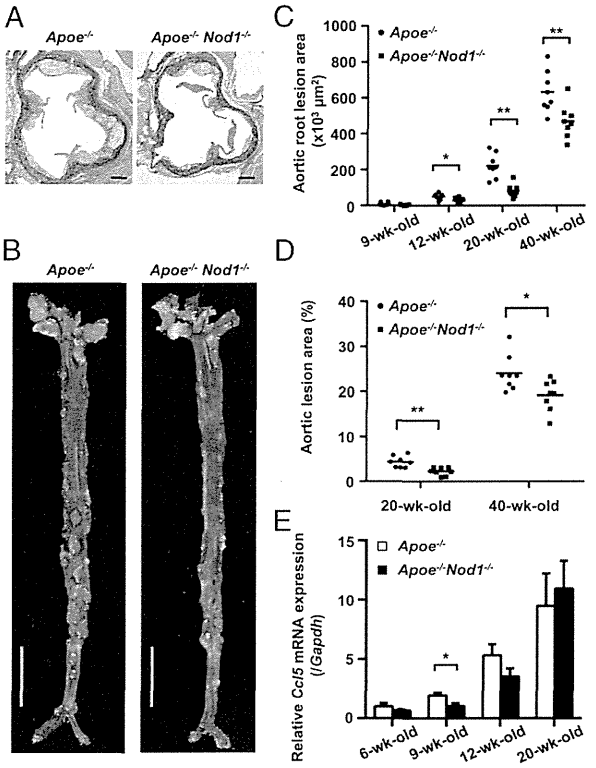

FIGURE 5. Development of atherosclerosis in Apoe$^{-/-}$ and Apoe$^{-/-}$ Nod1$^{-/-}$ mice at 9–40 wk of age without administration of Nod1 ligand. (A) Representative aortic roots stained with EVG in Apoe$^{-/-}$ or Apoe$^{-/-}$ Nod1$^{-/-}$ mice at 20 wk of age. Scale bars, 200 mm. (B) Representative aortas stained with Sudan IV in Apoe$^{-/-}$ or Apoe$^{-/-}$ Nod1$^{-/-}$ mice at 40 wk of age. Scale bars, 500 mm. (C) Quantification of atherosclerotic lesion areas of aortic roots in Apoe$^{-/-}$ or Apoe$^{-/-}$ Nod1$^{-/-}$ mice at the age of 9, 12, 20, or 40 wk. Bars represent means (n = 6–8/group). (D) Quantification of atherosclerotic lesion areas of aortas in Apoe$^{-/-}$ or Apoe$^{-/-}$ Nod1$^{-/-}$ mice at the age of 20 or 40 wk. Bars represent means (n = 8/group). (E) RT-PCR analysis of Ccl5 gene in aortic roots of Apoe$^{-/-}$ or Apoe$^{-/-}$ Nod1$^{-/-}$ mice at the age of 6, 9, 12, and 20 wk. The gene expression was normalized to expression of Gapdh. Relative expression levels to the values observed in aortic root from 6-wk-old Apoe$^{-/-}$ mice are presented as mean 6 SEM (n = 5/group). *p , 0.05, **p , 0.01 versus Apoe$^{-/-}$ mice at the same age (Student t test).

Apoe$^{-/-}$ Nod1$^{-/-}$ mice were lower than those in their age-matched Apoe$^{-/-}$ mice, and the difference was statistically significant at 9 wk of age (Fig. 5E). These results suggested that Ccl5 plays crucial roles in the development of atherosclerosis during the early phase induced by Nod1 ligand.

Discussion

The present study has demonstrated that long-term oral administration of a pure synthetic Nod1 ligand accelerated the development and progression of atherosclerosis in Apoe$^{-/-}$ mice, independent of cholesterol or triglyceride levels in blood. Additionally, the complete loss of this receptor significantly decreased the size of atherosclerotic lesions, providing evidence of a solid relationship between NOD1 and atherosclerosis. Previously, only limited studies have shown the effect of NOD1 in the cardiovascular field (25, 26) or the involvement of NOD1 in vascular inflammation induced by C. pneumoniae (12). No prior study, however, has directly proven the association between NOD1 and atherosclerosis in vivo.

By transplantation experiments, the major effector cells of the Nod1 ligand were nonhematopoietic cells. This is consistent with the observation that NOD1 in nonhematopoietic cells plays a key role in activation of human endothelial cells, mediated by C. pneumoniae (12), the chronic or recurrent infection of which was reported to have a close relationship to the development of atherosclerosis (27). Alternatively, Levin et al. (28) showed that increased lipid intake in receptor-interacting protein 2 (Rip2)$^{2/2}$ macrophages resulted in increased atherosclerotic lesions in apolipoprotein B$^{2/2}$ low-density lipoprotein receptor$^{2/2}$ mice transplanted with Rip2$^{2/2}$ bone marrow. Myeloid-specific depletion of Nod1 showed no significant difference in plaque formation in our study, and myeloid-specific depletion of Nod2, but not Rip2, showed significant reduction in the lipid-rich necrotic area in low-density lipoprotein receptor$^{2/2}$ mice (29). Therefore, it is possible that Rip2$^{2/2}$ macrophages exert their effects mainly through the alteration of lipid metabolism rather than Nod1 or Nod2 signaling pathways.

The marked expression of Ccl5 mRNA gene in the Nod1-induced atherosclerotic lesions and the inhibitory effect of Met-RANTES on Nod1-induced acceleration of atherosclerosis demonstrated that Ccl5 expression might be pathophysiologically important for the development and/or advancement of atherosclerosis. Consistent with the previous report that Ccl5 expression was most marked in early plaque (24), the effect of Nod1 for plaque formation appeared to be dominant at early stage (, 12 wk) because there was a marked downregulation of Ccl5 expression at that stage in Apoe$^{2/2}$ Nod1$^{2/2}$ mice. Ccl5 is a proinflammatory chemokine that regulates the trafficking of leukocytes such as macrophages and Th1 T cells, mediated by activation of the receptors Ccr1, Ccr3, Ccr4, and Ccr5 (30). In atherosclerosis, Ccr5 is known to be involved, not only in the recruitment of mononuclear cell, but also in the modulation of the immune balance (18, 31–33). Similarly, in FK565-administered Apoe$^{2/2}$ mice, Met-RANTES administration attenuated the infiltration of MOMA-2^{+} macrophages and CD3^{+} T cells in atherosclerotic lesions, suggesting that accumulation of both cell types by Ccl5 plays a role in Nod1-induced acceleration of atherosclerosis.

It has been reported that chronic or repeated infection was a strong risk factor for the development and aggravation of atherosclerosis (27, 34–36). However, it was difficult to show direct evidence of existing microorganisms in atherosclerotic plaques. Several studies showed the bacterial PGNs or DNA fragments existing in atherosclerotic plaques (37–39), and the metagenomic analysis of gut microbiome in patients with symptomatic atherosclerotic plaques and healthy controls demonstrated that patient metagenomes were enriched in genes encoding PGN biosynthesis (40). Furthermore, a recent report demonstrated that PGNs from microbiota were detected in systemically circulating blood, and they modulated the innate immune system through Nod1 (41). In the present study, we have demonstrated that Nod1 ligand directly contributed to the development of atherosclerosis. Taken together, systemically circulating PGN fragments from endogenous microbiota may activate Nod1-expressing vascular cells to produce various chemokines, including Ccl5, to promote the accumulation of inflammatory cells in the plaques and eventually accelerate the atherosclerotic formation in vessels. Although endogenous Nod1 ligands are still unknown, it is possible that yet-undetermined endogenous Nod1 ligands contribute to the development of atherosclerosis, because there are several studies that endogenous ligands toward other PRRs such as Tlr2, Tlr4, and Nlrp3 were involved in the acceleration of atherosclerosis (11, 42–45).

A recent study showed that gut flora influenced the nutrient processing and the metabolism in mice, and microbial processing of dietary choline was significantly correlated with atherosclerosis (46). Although it is still controversial whether Nod1 deficiency contributes to alteration of the composition of microflora (47, 48), alteration of the microbiota by Nod1 deficiency might play a role in the decreased development of atherosclerosis in Apoe$^{2/2}$ Nod1$^{2/2}$ mice. Because oral administration of FK565 might influence microbiota in the long-term observation, further investigation is needed on a role of microbiota in the acceleration of atherosclerosis through Nod1 activation.

In the previous studies, endogenous and synthetic ligands for Tlr2 and Tlr4 influenced the formation of atherosclerosis in addition to Nod1 (7, 9, 49). We found that Nod1 deficiency significantly reduced plaque formation by 50% in the aortas of 20-wk-old Apoe$^{2/2}$ mice, indicating that the contribution of Nod1 on atherogenesis is as strong as those of Tlr2 and Tlr4 suggested by the previous study (49). Interestingly, the effect of Nod1 for plaque formation seemed to be dominant at early stage (, 12 wk) as shown by marked downregulation of Ccl5 expression in Nod1$^{2/2}$ mice. Hence, it is possible that the ligand-specific effects of innate immune-mediated atherosclerosis formation might exist, and various types of ligands from microbiota would independently or synergistically work together for the development of atherosclerosis.

In conclusion, Nod1 activation plays one of the key roles in the development and progression of atherosclerosis. Further comprehensive studies on the innate immune ligand-specific contribution are necessary to understand the pathogenesis of atherosclerosis.

Acknowledgments

We are thankful to H. Fujii and C. Arimatsu for technical assistance, J. Kishimoto for statistical analyses, and Y. Nakashima for planning advice.

Disclosures

The authors have no financial conflicts of interest.

References

1. Ross, R. 1999. Atherosclerosis—an inflammatory disease. N. Engl. J. Med. 340: 115–126.
2. Packard, R. R., E. Maganto-García, I. Gotsman, I. Tabas, P. Libby, and A. H. Lichtman. 2008. CD11c^{+} dendritic cells maintain antigen processing, presentation capabilities, and CD4^{+} T-cell priming efficacy under hypercholesterolemic conditions associated with atherosclerosis. Circ. Res. 103: 965–973.
3. Zhou, X., A. Nicoletti, R. Elhage, and G. K. Hansson. 2000. Transfer of CD4^{+} T cells aggravates atherosclerosis in immunodeficient apolipoprotein E knockout mice. Circulation 102: 2919–2922.
4. Edfeldt, K., J. Swedenborg, G. K. Hansson, and Z. Q. Yan. 2002. Expression of Toll-like receptors in human atherosclerotic lesions: a possible pathway for plaque activation. Circulation 105: 1158–1161.
5. Naiki, Y., R. Sorrentino, M. H. Wong, K. S. Michelsen, K. Shimada, S. Chen, A. Yilmaz, A. Slepenkin, N. W. J. Schröder, T. R. Crother, et al. 2008. TLR/MyD88 and liver X receptor a signaling pathways reciprocally control Chlamydia pneumoniae-induced acceleration of atherosclerosis. J. Immunol. 181: 7176–7185.
6. Gibson, F. C., III, C. Hong, H. H. Chou, H. Yumoto, J. Chen, E. Lien, J. Wong, and C. A. Genco. 2004. Innate immune recognition of invasive bacteria accelerates atherosclerosis in apolipoprotein E-deficient mice. Circulation 109: 2801–2806.
7. Mullick, A. E., P. S. Tobias, and L. K. Curtiss. 2005. Modulation of atherosclerosis in mice by Toll-like receptor 2. J. Clin. Invest. 115: 3149–3156.
8. Takeuchi, O., and S. Akira. 2010. Pattern recognition receptors and inflammation. Cell 140: 805–820.
9. Michelsen, K. S., M. H. Wong, P. K. Shah, W. Zhang, J. Yano, T. M. Doherty, S. Akira, T. B. Rajavashisth, and M. Arditi. 2004. Lack of Toll-like receptor 4 or myeloid differentiation factor 88 reduces atherosclerosis and alters plaque phenotype in mice deficient in apolipoprotein E. Proc. Natl. Acad. Sci. USA 101: 10679–10684.
10. Björkbacka, H., V. V. Kunjathoor, K. J. Moore, S. Koehn, C. M. Ordija, M. A. Lee, T. Means, K. Halmen, A. D. Luster, D. T. Golenbock, and M. W. Freeman. 2004. Reduced atherosclerosis in MyD88-null mice links elevated serum cholesterol levels to activation of innate immunity signaling pathways. Nat. Med. 10: 416–421.
11. Duewell, P., H. Kono, K. J. Rayner, C. M. Sirois, G. Vladimer, F. G. Bauernfeind, G. S. Abela, L. Franchi, G. Nuñez, M. Schnurr, et al. 2010.

NLRP3 inflammasomes are required for atherogenesis and activated by cholesterol crystals. Nature 464: 1357–1361.
12. Opitz, B., S. Förster, A. C. Hocke, M. Maass, B. Schmeck, S. Hippenstiel, N. Suttorp, and M. Krüll. 2005. Nod1-mediated endothelial cell activation by Chlamydophila pneumoniae. Circ. Res. 96: 319–326.
13. Girardin, S. E., I. G. Boneca, L. A. M. Carneiro, A. Antignac, M. Jéhanno, J. Viala, K. Tedin, M. K. Taha, A. Labigne, U. Zähringer, et al. 2003. Nod1 detects a unique muropeptide from gram-negative bacterial peptidoglycan. Science 300: 1584–1587.
14. Inohara, N., T. Koseki, L. del Peso, Y. Hu, C. Yee, S. Chen, R. Carrio, J. Merino, D. Liu, J. Ni, and G. Núñez. 1999. Nod1, an Apaf-1-like activator of caspase-9 and nuclear factor-kB. J. Biol. Chem. 274: 14560–14567.
15. Bertin, J., W. J. Nir, C. M. Fischer, O. V. Tayber, P. R. Errada, J. R. Grant, J. J. Keilty, M. L. Gosselin, K. E. Robison, G. H. Wong, et al. 1999. Human CARD4 protein is a novel CED-4/Apaf-1 cell death family member that activates NF-kB. J. Biol. Chem. 274: 12955–12958.
16. Nishio, H., S. Kanno, S. Onoyama, K. Ikeda, T. Tanaka, K. Kusuhara, Y. Fujimoto, K. Fukase, K. Sueishi, and T. Hara. 2011. Nod1 ligands induce site-specific vascular inflammation. Arterioscler. Thromb. Vasc. Biol. 31: 1093–1099.
17. Shigeoka, A. A., A. Kambo, J. C. Mathison, A. J. King, W. F. Hall, J. da Silva Correia, R. J. Ulevitch, and D. B. McKay. 2010. Nod1 and Nod2 are expressed in human and murine renal tubular epithelial cells and participate in renal ischemia reperfusion injury. J. Immunol. 184: 2297–2304.
18. Veillard, N. R., B. Kwak, G. Pelli, F. Mulhaupt, R. W. James, A. E. Proudfoot, and F. Mach. 2004. Antagonism of RANTES receptors reduces atherosclerotic plaque formation in mice. Circ. Res. 94: 253–261.
19. Goossens, P., M. J. Gijbels, A. Zernecke, W. Eijgelaar, M. N. Vergouwe, I. van der Made, J. Vanderlocht, L. Beckers, W. A. Buurman, M. J. Daemen, et al. 2010. Myeloid type I interferon signaling promotes atherosclerosis by stimulating macrophage recruitment to lesions. Cell Metab. 12: 142–153.
20. Liou, J. T., C. C. Mao, D. Ching-Wah Sum, F. C. Liu, Y. S. Lai, J. C. Li, and Y. J. Day. 2013. Peritoneal administration of Met-RANTES attenuates inflammatory and nociceptive responses in a murine neuropathic pain model. J. Pain 14: 24–35.
21. Reikvam, D. H., A. Erofeev, A. Sandvik, V. Grcic, F. L. Jahnsen, P. Gaustad, K. D. McCoy, A. J. Macpherson, L. A. Meza-Zepeda, and F. E. Johansen. 2011. Depletion of murine intestinal microbiota: effects on gut mucosa and epithelial gene expression. PLoS ONE 6: e17996.
22. Paigen, B., A. Morrow, P. A. Holmes, D. Mitchell, and R. A. Williams. 1987. Quantitative assessment of atherosclerotic lesions in mice. Atherosclerosis 68: 231–240.
23. Nakashima, Y., A. S. Plump, E. W. Raines, J. L. Breslow, and R. Ross. 1994. ApoE-deficient mice develop lesions of all phases of atherosclerosis throughout the arterial tree. Arterioscler. Thromb. 14: 133–140.
24. Lutgens, E., B. Faber, K. Schapira, C. T. Evelo, R. van Haaften, S. Heeneman, K. B. Cleutjens, A. P. Bijnens, L. Beckers, J. G. Porter, et al. 2005. Gene profiling in atherosclerosis reveals a key role for small inducible cytokines: validation using a novel monocyte chemoattractant protein monoclonal antibody. Circulation 111: 3443–3452.
25. Cartwright, N., O. Murch, S. K. McMaster, M. J. Paul-Clark, D. A. van Heel, B. Ryffel, V. F. Quesniaux, T. W. Evans, C. Thiemermann, and J. A. Mitchell. 2007. Selective NOD1 agonists cause shock and organ injury/dysfunction in vivo. Am. J. Respir. Crit. Care Med. 175: 595–603.
26. Moreno, L., S. K. McMaster, T. Gatheral, L. K. Bailey, L. S. Harrington, N. Cartwright, P. C. Armstrong, T. D. Warner, M. Paul-Clark, and J. A. Mitchell. 2010. Nucleotide oligomerization domain 1 is a dominant pathway for NOS2 induction in vascular smooth muscle cells: comparison with Toll-like receptor 4 responses in macrophages. Br. J. Pharmacol. 160: 1997–2007.
27. Maass, M., C. Bartels, P. M. Engel, U. Mamat, and H. H. Sievers. 1998. Endovascular presence of viable Chlamydia pneumoniae is a common phenomenon in coronary artery disease. J. Am. Coll. Cardiol. 31: 827–832.
28. Levin, M. C., P. Jirholt, A. Wramstedt, M. E. Johansson, A. M. Lundberg, M. G. Trajkovska, M. Ståhlman, P. Fogelstrand, M. Brisslert, L. Fogelstrand, et al. 2011. Rip2 deficiency leads to increased atherosclerosis despite decreased inflammation. Circ. Res. 109: 1210–1218.
29. Johansson, M. E., X. Y. Zhang, K. Edfeldt, A. M. Lundberg, M. C. Levin, J. Borén, W. Li, X. M. Yuan, L. Folkersen, P. Eriksson, et al. 2014. Innate immune receptor NOD2 promotes vascular inflammation and formation of lipid-rich necrotic cores in hypercholesterolemic mice. Eur. J. Immunol. 44: 3081–3092.
30. Appay, V., and S. L. Rowland-Jones. 2001. RANTES: a versatile and controversial chemokine. Trends Immunol. 22: 83–87.
31. Weber, C., and H. Noels. 2011. Atherosclerosis: current pathogenesis and therapeutic options. Nat. Med. 17: 1410–1422.
32. Braunersreuther, V., A. Zernecke, C. Arnaud, E. A. Liehn, S. Steffens, E. Shagdarsuren, K. Bidzhekov, F. Burger, G. Pelli, B. Luckow, et al. 2007. Ccr5 but not Ccr1 deficiency reduces development of diet-induced atherosclerosis in mice. Arterioscler. Thromb. Vasc. Biol. 27: 373–379.
33. Potteaux, S., C. Combadière, B. Esposito, C. Lecureuil, H. Ait-Oufella, R. Merval, P. Ardouin, A. Tedgui, and Z. Mallat. 2006. Role of bone marrow-derived CC-chemokine receptor 5 in the development of atherosclerosis of low-density lipoprotein receptor knockout mice. Arterioscler. Thromb. Vasc. Biol. 26: 1858–1863.
34. Saikku, P., M. Leinonen, L. Tenkanen, E. Linnanmäki, M. R. Ekman, V. Manninen, M. Mänttäri, M. H. Frick, and J. K. Huttunen. 1992. Chronic Chlamydia pneumoniae infection as a risk factor for coronary heart disease in the Helsinki Heart Study. Ann. Intern. Med. 116: 273–278.
35. Chiu, B., E. Viira, W. Tucker, and I. W. Fong. 1997. Chlamydia pneumoniae, cytomegalovirus, and herpes simplex virus in atherosclerosis of the carotid artery. Circulation 96: 2144–2148.
36. Kiechl, S., G. Egger, M. Mayr, C. J. Wiedermann, E. Bonora, F. Oberhollenzer, M. Muggeo, Q. Xu, G. Wick, W. Poewe, and J. Willeit. 2001. Chronic infections and the risk of carotid atherosclerosis: prospective results from a large population study. Circulation 103: 1064–1070.
37. Laman, J. D., A. H. Schoneveld, F. L. Moll, M. van Meurs, and G. Pasterkamp. 2002. Significance of peptidoglycan, a proinflammatory bacterial antigen in atherosclerotic arteries and its association with vulnerable plaques. Am. J. Cardiol. 90: 119–123.
38. Ott, S. J., N. E. El Mokhtari, M. Musfeldt, S. Hellmig, S. Freitag, A. Rehman, T. Kühbacher, S. Nikolaus, P. Namsolleck, M. Blaut, et al. 2006. Detection of diverse bacterial signatures in atherosclerotic lesions of patients with coronary heart disease. Circulation 113: 929–937.
39. Koren, O., A. Spor, J. Felin, F. Fåk, J. Stombaugh, V. Tremaroli, C. J. Behre, R. Knight, B. Fagerberg, R. E. Ley, and F. Bäckhed. 2011. Human oral, gut, and plaque microbiota in patients with atherosclerosis. Proc. Natl. Acad. Sci. USA 108(Suppl. 1): 4592–4598.
40. Karlsson, F. H., F. Fåk, I. Nookaew, V. Tremaroli, B. Fagerberg, D. Petranovic, F. Bäckhed, and J. Nielsen. 2012. Symptomatic atherosclerosis is associated with an altered gut metagenome. Nat. Commun. 3: 1245.
41. Clarke, T. B., K. M. Davis, E. S. Lysenko, A. Y. Zhou, Y. Yu, and J. N. Weiser. 2010. Recognition of peptidoglycan from the microbiota by Nod1 enhances systemic innate immunity. Nat. Med. 16: 228–231.
42. Ohashi, K., V. Burkart, S. Flohé, and H. Kolb. 2000. Cutting edge: heat shock protein 60 is a putative endogenous ligand of the toll-like receptor-4 complex. J. Immunol. 164: 558–561.
43. Kanwar, R. K., J. R. Kanwar, D. Wang, D. J. Ormrod, and G. W. Krissansen. 2001. Temporal expression of heat shock proteins 60 and 70 at lesion-prone sites during atherogenesis in ApoE-deficient mice. Arterioscler. Thromb. Vasc. Biol. 21: 1991–1997.
44. Smiley, S. T., J. A. King, and W. W. Hancock. 2001. Fibrinogen stimulates macrophage chemokine secretion through Toll-like receptor 4. J. Immunol. 167: 2887–2894.
45. Okamura, Y., M. Watari, E. S. Jerud, D. W. Young, S. T. Ishizaka, J. Rose, J. C. Chow, and J. F. Strauss, III. 2001. The extra domain A of fibronectin activates Toll-like receptor 4. J. Biol. Chem. 276: 10229–10233.
46. Koeth, R. A., Z. Wang, B. S. Levison, J. A. Buffa, E. Org, B. T. Sheehy, E. B. Britt, X. Fu, Y. Wu, L. Li, et al. 2013. Intestinal microbiota metabolism of L-carnitine, a nutrient in red meat, promotes atherosclerosis. Nat. Med. 19: 576–585.
47. Bouskra, D., C. Brézillon, M. Bérard, C. Werts, R. Varona, I. G. Boneca, and G. Eberl. 2008. Lymphoid tissue genesis induced by commensals through NOD1 regulates intestinal homeostasis. Nature 456: 507–510.
48. Robertson, S. J., J. Y. Zhou, K. Geddes, S. J. Rubino, J. H. Cho, S. E. Girardin, and D. J. Philpott. 2013. Nod1 and Nod2 signaling does not alter the composition of intestinal bacterial communities at homeostasis. Gut Microbes 4: 222–231.
49. Higashimori, M., J. B. Tatro, K. J. Moore, M. E. Mendelsohn, J. B. Galper, and D. Beasley. 2011. Role of Toll-like receptor 4 in intimal foam cell accumulation in apolipoprotein E-deficient mice. Arterioscler. Thromb. Vasc. Biol. 31: 50–57.

9. Gong YY, Xie L, Zhou WP et al. Glucose and lipid profile of a long-lived rural Han Chinese population and their families in southwest China. J Am Geriatr Soc 2009;57:567–568.
10. Ye JJ, Li JC, Peng L et al. Nonagenarians and centenarians in a rural Han Chinese population: Lifestyle and epidemics. J Am Geriatr Soc 2009; 57:1723–1724.

Case Reports

ENDOCRINE AND METABOLIC ABNORMALITIES IN A GIRL WITH CHILDHOOD WERNER SYNDROME: CASE REPORT

To the Editor: Werner syndrome (WS) is a rare progeroid syndrome of autosomal-recessive inheritance that German ophthalmologist Otto Werner first reported in 1904. The frequency of WS is as high as 1 in 40,000 in Japan, with consanguineous marriage noted in approximately 40% of cases, although no regional localization of cases has been recognized.[1,2] Most progeroid phenotypes are clinically typical, including the graying and loss of hair; hoarseness and scleroderma-like skin changes emerging in the 20s; and juvenile cataracts, insulin-resistant diabetes mellitus, hypogonadism, ulceration of the skin, osteoporosis, and soft tissue calcification arising in the 30s. The most severe and lethal conditions are malignant tumors and cardiovascular or cerebrovascular diseases resulting from premature atherosclerosis in the 40s and 50s.[1–4] Mean age at diagnosis was 36.7 in individuals who presented with typical signs of WS.[3] In contrast, individuals who develop the disease in childhood are not usually reported primarily because of the variety of nonspecific symptoms and lack of cardinal signs during the teenage years. The case of a girl diagnosed with WS at 17 is herein reported.

The girl's parents were second cousins without a family history suggesting the presence of genetic diseases, including progeroid syndromes. The girl was healthy at birth and exhibited normal growth and development in infancy. Starting at 6 years old, she gradually developed facial erythema (Figure 1) and failure to grow. At 10 years old, her parents consulted a pediatrician regarding her growth failure and chronic fatigue of unknown etiology. Clinical and laboratory examinations identified a diagnosis of hypothyroidism, and levothyroxine treatment was started, but she discontinued the medication after several months. At 17 years old, she again consulted a physician and was referred to the hospital for systematic evaluation.

She was 141 cm (3.3 standard deviations below the mean) tall and weighed 33.2 kg (2.7 standard deviations below the mean), and her body mass index was 16.7 kg/m^2. She had slightly gray hair, erythema on both cheeks, and dry skin over her entire body. Laboratory findings demonstrated hepatic dysfunction (aspartate aminotransferase, 132 U/L (normal range (NR) 13–33 U/L); alanine aminotransferase, 252 U/L (NR 6–30 U/L); gamma-glutamyl transpeptidase, 51 U/L (NR 10–47 U/L)) and dyslipidemia (triglycerides, 221 mg/dL (NR, 30–149 mg/dL); low-density lipoprotein cholesterol, 140 mg/dL (NR <139)), with normal serum creatine phosphokinase, blood urea nitrogen, and creatinine levels. Metabolic and endocrinological studies revealed hypothyroidism (basal thyroid-stimulating hormone (TSH), 11.22 l U/mL (NR 0.27–4.20 l U/mL); free thyroxine, 0.82 ng/dL (NR 1.00–1.80 ng/dL)) with a remarkably high TSH level after a thyrotropin releasing hormone loading test (58.48 l U/mL at 60 minutes (NR 10–25 l U/mL)). An oral glucose tolerance test with 75-g oral glucose loading showed borderline glucose intolerance with remarkable insulin resistance (blood glucose, 197 mg/dL (NR 60–125 mg/dL); insulin, 563 l U/mL at 120 minutes (NR <300)). Ultrasonography demonstrated an atrophic thyroid and marked fatty liver. Brachial–ankle pulse wave velocity indicated slight arteriosclerotic changes (right 1,188 cm/s, left 1,157 cm/s, mean 952 ± 103 cm/s). Bilateral ovary hypoplasia and a right ovarian cyst were detected on magnetic resonance imaging. Ophthalmological study revealed bilateral cataracts. There were no signs of osteoporosis of the lumbar spine (bone mineral density 0.968 g/cm^3; Z-score −0.4). No calcification of the Achilles tendon, a cardinal sign of WS in adulthood,[1] was detected on X-ray examination. Genetic tests identified a homozygous mutation of IVS25–1G>C in the WRN gene, one of the most common mutations in Japanese individuals with WS. Medical treatment with levothyroxine sodium hydrate at a dose of 100 l g/d quickly normalized the girl's thyroid function, with an associated increase in her vigor. Subsequent biguanide therapy (750 mg/d) was discontinued within 1 week because of abdominal pain.

Figure 1. Facial erythema and beak-like appearance.

Based on the clinical features reported in previous studies, the characteristic abnormalities in metabolism observed in individuals with WS are mainly attributed to peripheral lipoatrophy with insulin insensitivity or dyslipidemia.[5] Endocrinological problems in the setting of WS primarily derive from the impaired secretion of hormones due to premature aging of endocrine organs, and empirically, hypogonadism, hypothyroidism, and hypopituitarism are the major endocrinological concerns in individuals with WS. Although these conditions may be present in childhood, no clinical studies have reported such features, probably because of the difficulty in diagnosing WS in individuals with nonspecific symptoms. The present case therefore provides important and valuable information. First, hypothyroidism of atrophic thyroid glands in addition to pituitary and hypothalamic dysfunction can appear as early as 10 years of age. Second, marked insulin insensitivity due to a lipodystrophic phenotype can arise in

adolescence. Third, the subject gradually exhibited hypergonadotrophic hypogonadism in her teens. Hence, nonspecific metabolic and endocrinological conditions, as well as atrophic skin, growth failure, and bilateral cataracts, may be characteristic findings of WS in childhood. According to previous reports,[2] an earlier onset of clinical symptoms is associated with a shorter life span. Hence, it is critically important to make a proper diagnose at an early age to initiate careful and consistent observation and provide early therapeutic intervention.

Naoko Toda, MD
Kenji Ihara, MD, PhD
Department of Pediatrics, Graduate School of Medical Sciences, Kyushu University, Fukuoka, Japan

Minoru Takemoto, MD, PhD
Koutaro Yokote, MD, PhD
Department of Clinical Cell Biology and Medicine Graduate School of Medicine, Chiba University, Chiba Japan

Toshiro Hara, MD, PhD
Department of Pediatrics, Graduate School of Medical Sciences, Kyushu University, Fukuoka, Japan

ACKNOWLEDGMENTS

Conflict of Interest: The editor-in-chief has reviewed the conflict of interest checklist provided by the authors and has determined that the authors have no financial or any other personal conflicts with respect to this work.

Author Contributions: Study concept and design: Toda, Ihara. Acquisition of subject and data: Toda, Ihara. Study design and interpretation of the data: Watanabe, Takemoto, Yokote. Preparation of manuscript: Toda, Ihara.

Sponsor's Role: No sponsors.

REFERENCES

1. Takemoto M, Mori S, Kuzuya M et al. Diagnostic criteria for Werner syndrome based on Japanese nationwide epidemiological survey. Geriatr Gerontol Int 2013;13:475–481.
2. Goto M, Ishikawa Y, Sugimoto M et al. Werner syndrome: A changing pattern of clinical manifestations in Japan (1917–2008). Biosci Trends 2013;7:13–22.
3. Goto M. Hierarchical deterioration of body systems in Werner's syndrome: Implications for normal ageing. Mech Ageing Dev 1997;98:239–254.
4. Lauper JM, Krause A, Vaughan TL et al. Spectrum and risk of neoplasia in Werner syndrome: A systematic review. PLoS ONE 2013;8:e59709.
5. Donadille B, D'Anella P, Auclair M et al. Partial lipodystrophy with severe insulin resistance and adult progeria Werner syndrome. Orphanet J Rare Dis 2013;8:106.

ONCE-WEEKLY TOLVAPTAN FOR CHRONIC SYMPTOMATIC HYPONATREMIA DUE TO SYNDROME OF INAPPROPRIATE SECRETION OF ANTI-DIURETIC HORMONE

To the Editor: An 83-year-old man was diagnosed with syndrome of inappropriate secretion of anti-diuretic hormone (SIADH) in 2009, when he developed severe symptomatic hyponatremia (sodium 119 mmol/L) after a respiratory tract infection. He was taking levothyroxine for hypothyroidism. He was unable to tolerate demeclocycline because he had hepatitis, and since then, his sodium had been maintained at approximately 125 mmol/L with fluid restriction. In December 2011, he fell and fractured his hip. At that time, his sodium was 123 mmol/L. He had a hemiarthroplasty and was hospitalized for 6 weeks.

In February 2012, he was admitted after a seizure. Laboratory tests showed sodium 118 mmol/L, urea 5.2 mmol/L, and creatinine 62 l mol/L. Despite strict fluid restriction, his sodium did not improve, and he remained confused and disoriented. He was started on tolvaptan 15 mg on alternate days to avoid rapid correction. He had profuse diuresis, and by Day 4 (just after two doses), his sodium had increased to 133 mmol/L and his urea from 5 to 16 mmol/L, and his symptoms had improved dramatically.

To avoid overcorrection and renal failure, tolvaptan was stopped, and fluid restriction was restarted, but his sodium fell to 119 mmol/L, and his symptoms returned within 2 days, so it was decided to try tolvaptan once a week. To avoid wide fluctuations in his sodium, he was advised to drink until thirst is eliminated for 4 days after taking tolvaptan and to restrict his fluids 3 days before the next dose. His sodium increased by 2 to 3 mmol/L per day for 3 days after tolvaptan and fell by 1 to 2 mmol/L per day after Day 3, and he remained symptom free.

After discharge, he took tolvaptan 15 mg once a week for 12 months and then 15 mg every 6 days because of tiredness and lethargy returning 5 days after taking tolvaptan. During this period, his sodium fluctuated around 125 mmol/L (range 122–133 mmol/L; Figure 1). Despite the fluctuation in his sodium, he remained asymptomatic and had not been admitted to the hospital. In February 2014, he was admitted with sepsis and died of multiorgan failure nearly 2 years after taking tolvaptan.

Hyponatremia is the most frequent electrolyte imbalance in elderly adults, and severe hyponatremia (sodium < 125 mmol/L) is found in up to 6% of hospitalized older adults.[1] Hyponatremia due to SIADH is often chronic and asymptomatic, but sodium levels of less than 125 mmol/L can cause unsteadiness, falls, attention deficit, and fractures in elderly adults.[2,3] Even though fluid restriction is effective, it is difficult to sustain over the long term.

Tolvaptan is a vasopressin receptor antagonist and is effective in the treatment of hyponatremia due to SIADH by promoting free water excretion.[4–6] Adverse effects include thirst, dehydration, and too-rapid correction of sodium (which can lead to complications). In clinical trials, 7% of participants had an increase in serum sodium of 8 mmol/L at 8 hours, and 2% had an increase of more than 12 mmol/L at 24 hours.[6]

The major constraints in using this drug are its cost, rapid correction with the risk of osmotic demyelination syndrome, rebound hyponatremia after stopping the drug, and uncertainty regarding long-term use.

Concerns have also been raised in using this drug over the long term because it could cause liver injury, and the Food and Drug Administration has warned that tolvaptan

Clin Pediatr Endocrinol 2014; 23(2), 59–64

Case Report

Thyroid Follicular Carcinoma in a Fourteen-year-old Girl with Graves' Disease

Kanako Kojima-Ishii[1], Kenji Ihara[1], Kazuhiro Ohkubo[1], Terumichi Matsuo[1], Naoko Toda[1], Hiroyuki Yamashita[2], Shinji Kono[3], and Toshiro Hara[1]

[1]*Department of Pediatrics, Graduate School of Medical Science, Kyushu University, Fukuoka, Japan*

[2]*Yamashita Thyroid and Parathyroid Clinic, Fukuoka, Japan*

[3]*Harasanshin Hospital, Fukuoka, Japan*

Abstract. Here we present the case of a 14-yr-old girl who developed thyroid follicular carcinoma accompanied by Graves' disease. She was diagnosed with Graves' disease at 10 yr of age and soon achieved a euthyroid state after starting treatment. When she was 13 yr of age, her hyperthyroidism and goiter worsened despite medical therapy. Multiple nodules were found in her enlarged thyroid gland by ultrasonography. Her serum Tg level seemed within the normal range. She underwent near-total thyroidectomy for control of thyroid function. Histopathological study demonstrated that multiple oxyphilic follicular neoplasms were surrounded by the thyroid tissue compatible with Graves' disease. Capsular invasion was identified in one of the nodules, and thus the histological diagnosis was minimally invasive follicular carcinoma. She did not have signs suggesting metastasis, and has had no relapse for 18 mo after the operation. Although some previous studies showed a high prevalence of thyroid cancer with an aggressive nature in adult patients with Graves' disease, few reports about thyroid cancer accompanied by Graves' disease are available in children. The present case, however, suggests that careful investigation is needed when we detect thyroid nodules or progressive thyroid enlargement, especially in children with Graves' disease.

Key words: Graves' disease, thyroid cancer

Introduction

Thyroid carcinoma is considered to be rare in childhood and adolescence (1). Histologically, most thyroid carcinomas are of the papillary type, with the follicular type accounting for 5% of cases (2). Although there have been a number of reports about thyroid carcinoma with Graves' disease in adult populations (3), few reports are available in children or adolescents (4, 5). Here we describe a 14-yr-old girl with thyroid follicular carcinoma unexpectedly found during the treatment of Graves' disease. Through the clinical features of this case, we reconfirmed the importance of careful investigation of the thyroid gland, especially in patients with Graves' disease and even in childhood or adolescence.

Received: December 9, 2013
Accepted: January 23, 2014
Corresponding Author: Dr. Kanako Kojima-Ishii, Department of Pediatrics, Graduate School of Medical Science, Kyushu University, 3-1-1 Maidashi, Higashi-ku, Fukuoka 814-8582, Japan
E-mail: k-kanako@momo.so-net.ne.jp

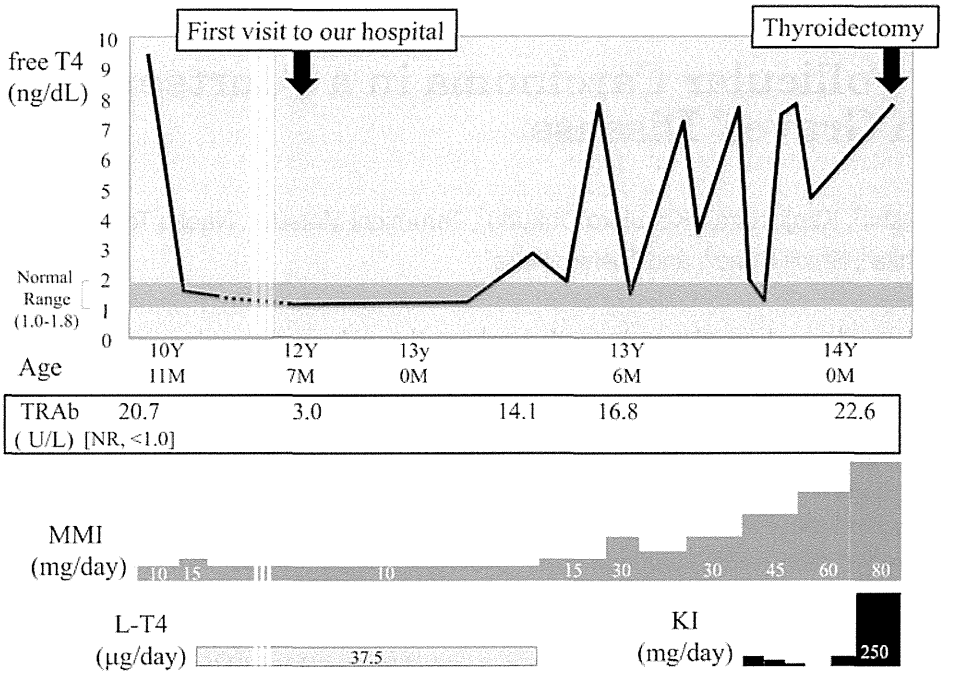

Fig. 1. Clinical course from onset until thyroidectomy. TRAb, TSH receptor antibody; MMI, thiamazole; L-T4, levothyroxine; KI, potassium iodine; NR, normal range.

Case Report

A 10-yr-old girl was brought to a hospital because of neck swelling. She was diagnosed with Graves' disease based on the findings of diffuse thyroid gland enlargement, hyperthyroidism and positive results for TSH receptor antibodies (free T3, >30 pg/mL [normal range (NR), 2.20–4.40]; free T4, 9.42 ng/dL [NR, 1.00–1.80]; TSH, <0.1 μU/mL [NR, 0.27–4.20]; TSH receptor antibody, 20.7 U/L [NR, <1.0]; thyroid stimulating antibody, 404% [NR, <180]). She had no history of appreciable diseases and no family history of thyroid diseases or early-onset cancers. Treatment with thiamazole (MMI) was started, and levothyroxine (L-T4) replacement was added subsequently. Her thyroid function was normalized within 2 mo, and the drug therapy was continued. When she was 12 yr old, she was referred to our hospital owing to a move with her family. At the first visit, we did not find swelling of her neck, and her thyroid hormone levels were within normal ranges, whereas she still showed positive antibody results (free T4 1.10 ng/dL, TSH 1.20 μU/mL, TSH receptor antibody 3.0 U/L). Her clinical course is shown in Fig. 1. We continued the therapy with MMI and L-T4, and then her clinical condition remained stable for 8 mo. At the age of 13 yr and 3 mo, her hyperthyroidism worsened and neck swelling began again. We stopped the L-T4, increased the dose of MMI up to 80 mg/d and added treatment with potassium iodine (KI), the final dose of which reached 250 mg/d. Despite the intensive medical therapy, her thyroid hormone levels remained above normal ranges. Laboratory findings at 13 yr and 11 mo of age are shown in Table 1. Her level of Tg seemed within the normal range, although the accuracy could not be evaluated because of a high level of serum TgAb. Her consciousness was clear and physical examination showed anterior neck swelling without a palpable tumor, finger tremor at rest and no heart murmur or arrhythmia by auscultation. Her blood pressure was 112/50

Table 1 Laboratory findings at 13 yr and 11 mo of age

WBC	4.33×10^3	μL	ALP	620	U/L	free T4	>7.77	ng/dL
Hb	12.2	g/dL	TC	111	mg/dL	free T3	>32.55	pg/mL
Plt	275×10^3	/μL	TG	73	mg/dL	TSH	<0.01	μU/mL
TP	6.2	g/dL	BS	105	mg/dL	TgAb	1273.5	U/mL
Alb	3.9	g/dL	CPK	66	U/L	TPOAb	1404	U/mL
BUN	13	mg/dL	CRP	0.01	mg/dL	TRAb	22.6	U/L
Cr	0.31	mg/dL	BNP	6.9	pg/mL	TSAb	800	%
AST	23	U/L				Tg	8.1	ng/mL
ALT	30	U/L						

TgAb, Tg antibody; TPOAb, thyroid peroxidase antibody; TRAb, TSH receptor antibody; TSAb, thyroid stimulating antibody.

mmHg and heart rate was 118/min. While she presented with severe hyperthyroidism with a high level of TSH receptor antibody, no symptoms suggestive of thyroid crisis were observed. Thyroid ultrasonography showed diffuse goiter and increased blood flow by Doppler analysis, and these findings were consistent with an active state of Graves' disease. In addition, we detected multiple nodules in both lobes, the diameters of which were 10–17 mm. One nodule in the right lobe had heterogeneous internal echogenicity and others showed homogeneous internal echogenicity. All of these nodules appeared to have regular margins without microcalcifications (Fig. 2). When she was 14 yr and 1 mo of age, she underwent near-total thyroidectomy to control thyroid function. The weight of the isolated thyroid gland was 105 g (right lobe 55 g, left lobe 50 g), and multiple nodules were seen in both lobes as detected by ultrasonography. Histopathological study showed multiple oxyphilic follicular neoplasms. Capsular invasion with full-thickness interruption of the capsule was detected in one of the nodules in the left lobe (Fig. 3). The tissue surrounding the nodules showed typical finding of Graves' disease. The histological diagnosis of the nodule was minimally invasive follicular carcinoma. Other nodules were not histologically qualified for carcinoma. Vascular invasion, or lymph node or distal metastases of tumor cells were not observed. At present, 18 mo after the surgery, she has no sign of relapse and maintains a euthyroid state with L-T4 replacement therapy.

Discussion

There are a number of reports about the association between Graves' disease and thyroid cancer in adult populations. According to a recent review, the prevalence of thyroid carcinoma in Graves' disease is 0.5–15.0% (3). A study in Italy showed that the annual incidence of thyroid carcinoma in Graves' disease was 175/100,000 (6), which seemed higher than the recently reported incidence of 9.1/100,000 in the general population of Japan (7). However, due to differences in clinical or histological criteria, genetic background and iodine availability among the studies, it remains a matter of debate whether the prevalence of thyroid carcinoma is higher in patients with Graves' disease. Besides, there are reports that thyroid carcinoma accompanied by Graves' disease had an aggressive nature and association with high mortality (3, 6, 8–10). On the other hand, some studies did not show high-grade malignant characteristics of thyroid cancer in Graves' disease (11, 12). Therefore, the prognosis of thyroid cancer with Graves' disease has also been controversial. The mechanisms of the possible malignant potential of thyroid cancer in Graves' disease have not been elucidated. In previous reports, anti-thyroid drugs (13), stimulating TSH receptor antibody (14) or locally produced interleukins (15) were speculated to be factors that modify tumor characteristics.

Thyroid cancer is very rare in children and adolescents. It reportedly accounts for

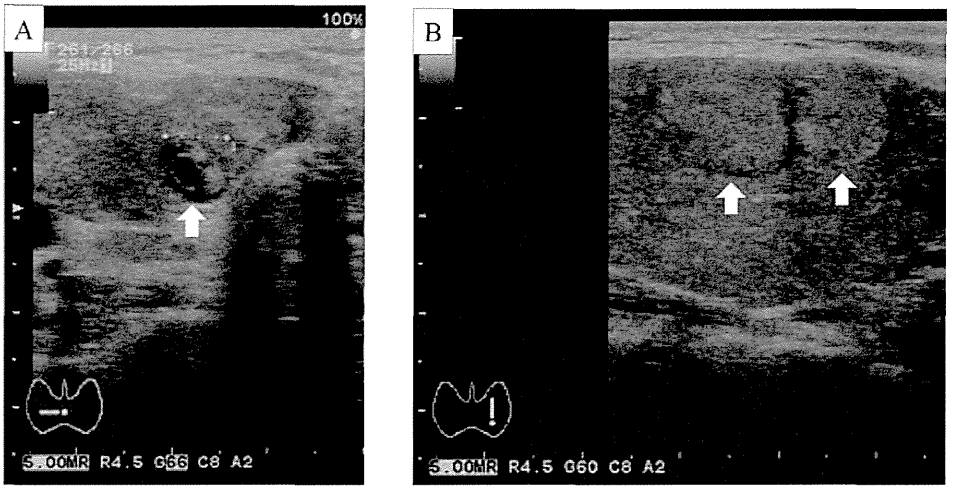

Fig. 2. Ultrasonographic thyroid images at 13 yr and 11 mo of age. Multiple nodules can be seen in both lobes. The diameters of the nodules range from 10 to 17 mm. The nodules did not have irregular margins or microcalcifications. A: Right lobe. B: Left lobe. The nodules are indicated by white arrows.

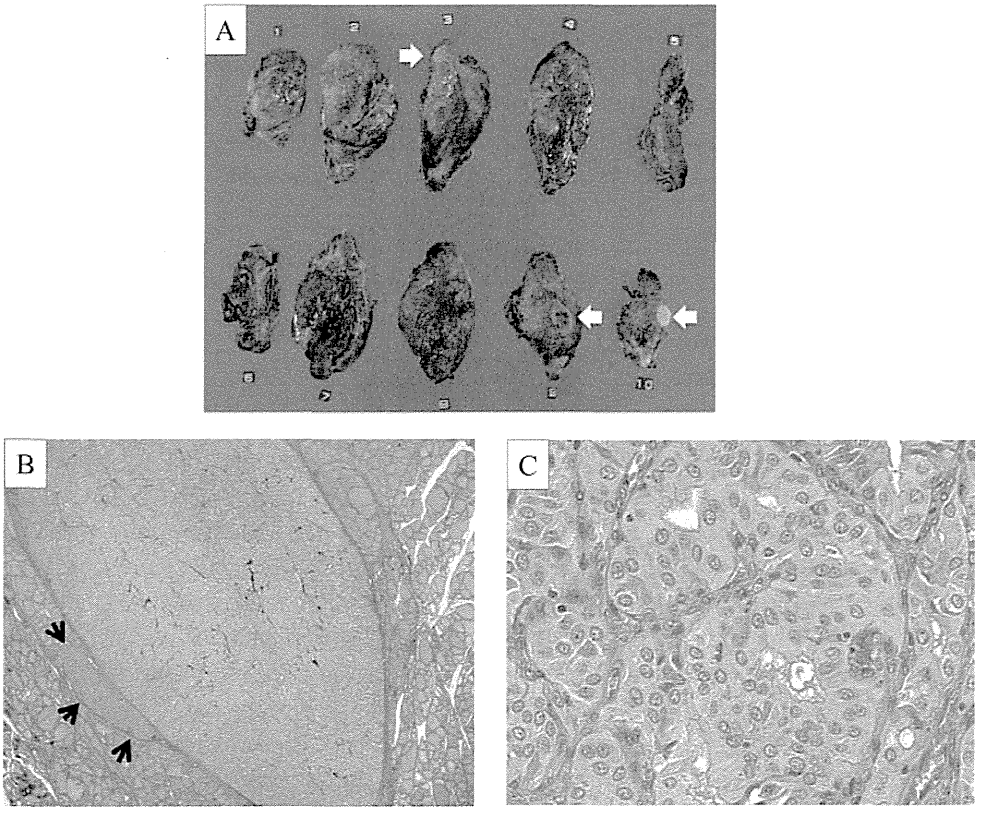

Fig. 3. Histological images of the thyroid grand. A: Macroscopic images of the isolated thyroid. Arrows indicate nodules in both lobes. B: Microscopic images (hematoxylin-eosin staining ×12.5). C: Microscopic images (hematoxylin-eosin staining ×600). Multiple oxyphilic follicular neoplasms can be seen. Capsular invasion is indicated by arrows in B. The thyroid tissue surrounding nodules is histologically normal with characteristic findings of Graves' disease.

approximately 0.5–3% of all carcinomas in their age groups (1), and its incidence under the age of 20 is about one in 100,000 in Japan (7). The prevalence of thyroid nodules in children was reported to be lower than that in adults (1, 16, 17). But some reports showed that the cancer risk of thyroid nodules is higher in children than in adults. In a review of 16 papers, the overall incidence of malignancy in thyroid nodules in children was 26.4% (18). On the other hand, a study of adults showed that the incidence of malignancy was 5.3% in cold thyroid nodules (19). In a recent study, the malignant risk of thyroid nodules was 22% in children, whereas it was 14% in adults (20). Thyroid cancer in pediatric populations has some specific characteristics, such as fast growing speed, high ratio of multifocal invasion and a tendency for metastasis and recurrence, although the overall survival rate of child patients was reported to be fairly high (2). Few children with thyroid cancer with Graves' disease have been reported. Niedziela *et al.* demonstrated a boy with thyroid papillary cancer accompanied by Graves' disease (4). Histologically, 90–95% of thyroid carcinomas are of the papillary type, and 5% are of the follicular type in all age groups (2). Therefore, the present case of thyroid follicular carcinoma with Graves' disease in a teenage girl was extraordinary rare. While no susceptibility genes have been identified for non-syndromic and non-medullary thyroid carcinoma, genetic alternations such as PAX8-PPAR gamma translocations or RAS mutations have been observed in thyroid follicular carcinoma (21). The present case had no familial history of any type of carcinoma; however, it might be possible that she had some genetic susceptibility to the onset of thyroid tumors and that a cancer-causing mutation, a so-called "second hit", occurred in a thyroid cell under stimulatory conditions through the TSH receptor as a result of organ-specific autoimmunity.

In this case, we did not think about the presence of thyroid cancer in the thyroid glands before thyroidectomy because clinical findings suggestive of coexisting malignancy were not observed. In general, characteristic findings of a malignant thyroid nodule by ultrasonography include irregular shape, ill-defined edge, jagged border, heterogeneous nature or microcalcifications (18, 22), whereas minimally invasive follicular carcinoma often does not show any of these findings (22). In this case, although one nodule had heterogeneous internal echoes, we did not see other malignant findings. Consequently, we assumed that the progressing thyroid enlargement was simply a symptom of Graves' disease. However, we should have evaluated the thyroid much more intensively in consideration of the ultrasound features and substantial risk for carcinogenesis in Graves' disease, especially in adolescence.

In conclusion, we reported a case of thyroid follicular carcinoma accompanied by Graves' disease in a 14-yr-old girl. Although thyroid cancer rarely occurs in pediatric populations, careful investigation is needed if we observe progressive thyroid enlargement or detect thyroid nodules by ultrasonography, even in children with Graves' disease.

References

1. Corrias A, Mussa A. Thyroid nodules in pediatrics: which ones can be left alone, which ones must be investigated, when and how. J Clin Res Pediatr Endocrinol 2013;5(Suppl 1):57–69. [Medline]
2. Vaisman F, Corbo R, Vaisman M. Thyroid carcinoma in children and adolescents-systematic review of the literature. J Thyroid Res 2011;2011:845362.
3. Pazaitou-Panayiotou K, Michalakis K, Paschke R. Thyroid cancer in patients with hyperthyroidism. Horm Metab Res 2012;44:255–62. [Medline] [CrossRef]
4. Niedziela M, Korman E. Thyroid carcinoma in a fourteen-year-old boy with Graves disease. Med Pediatr Oncol 2002;38:290–1. [Medline] [CrossRef]
5. Corrias A, Cassio A, Weber G, Mussa A, Wasniewska M, Rapa A, *et al.* Study Group for

Thyroid Diseases of Italian Society for Pediatric Endocrinology and Diabetology (SIEDP/ISPED) Thyroid nodules and cancer in children and adolescents affected by autoimmune thyroiditis. Arch Pediatr Adolesc Med 2008;162:526–31. [Medline] [CrossRef]
6. Pellegriti G, Belfiore A, Giuffrida D, Lupo L, Vigneri R. Outcome of differentiated thyroid cancer in Graves' patients. J Clin Endocrinol Metab 1998;83:2805–9. [Medline]
7. Matsuda A, Matsuda T, Shibata A, Katanoda K, Sobue T, Nishimoto H, Japan Cancer Surveillance Research Group Cancer incidence and incidence rates in Japan in 2007: a study of 21 population-based cancer registries for the Monitoring of Cancer Incidence in Japan (MCIJ) project. Jpn J Clin Oncol 2013;43:328–36. [Medline] [CrossRef]
8. Belfiore A, Garofalo MR, Giuffrida D, Runello F, Filetti S, Fiumara A, *et al.* Increased aggressiveness of thyroid cancer in patients with Graves' disease. J Clin Endocrinol Metab 1990;70:830–5. [Medline] [CrossRef]
9. Cappelli C, Braga M, De Martino E, Castellano M, Gandossi E, Agosti B, *et al.* Outcome of patients surgically treated for various forms of hyperthyroidism with differentiated thyroid cancer: experience at an endocrine center in Italy. Surg Today 2006;36:125–30. [Medline] [CrossRef]
10. Pellegriti G, Mannarino C, Russo M, Terranova R, Marturano I, Vigneri R, *et al.* Increased mortality in patients with differentiated thyroid cancer associated with Graves' disease. J Clin Endocrinol Metab 2013;98:1014–21. [Medline] [CrossRef]
11. Hales IB, McElduff A, Crummer P, Clifton-Bligh P, Delbridge L, Hoschl R, *et al.* Does Graves' disease or thyrotoxicosis affect the prognosis of thyroid cancer. J Clin Endocrinol Metab 1992;75:886–9. [Medline]
12. Yano Y, Shibuya H, Kitagawa W, Nagahama M, Sugino K, Ito K, *et al.* Recent outcome of Graves' disease patients with papillary thyroid cancer. Eur J Endocrinol 2007;157:325–9. [Medline] [CrossRef]
13. Dobyns BM, Sheline GE, Workman JB, Tompkins EA, McConahey WM, Becker DV. Malignant and benign neoplasms of the thyroid in patients treated for hyperthyroidism: a report of the cooperative thyrotoxicosis therapy follow-up study. J Clin Endocrinol Metab 1974;38:976–98. [Medline] [CrossRef]
14. Filetti S, Belfiore A, Amir SM, Daniels GH, Ippolito O, Vigneri R, *et al.* The role of thyroid-stimulating antibodies of Graves' disease in differentiated thyroid cancer. N Engl J Med 1988;318:753–9. [Medline] [CrossRef]
15. Vella V, Mineo R, Frasca F, Mazzon E, Pandini G, Vigneri R, *et al.* Interleukin-4 stimulates papillary thyroid cancer cell survival: implications in patients with thyroid cancer and concomitant Graves' disease. J Clin Endocrinol Metab 2004;89:2880–9. [Medline] [CrossRef]
16. Aghini-Lombardi F, Antonangeli L, Martino E, Vitti P, Maccherini D, Leoli F, *et al.* The spectrum of thyroid disorders in an iodine-deficient community: the Pescopagano survey. J Clin Endocrinol Metab 1999;84:561–6. [Medline]
17. Halac I, Zimmerman D. Thyroid nodules and cancers in children. Endocrinol Metab Clin North Am 2005;34:725–44. [Medline] [CrossRef]
18. Niedziela M. Pathogenesis, diagnosis and management of thyroid nodules in children. Endocr Relat Cancer 2006;13:427–53. [Medline] [CrossRef]
19. Belfiore A, La Rosa GL, La Porta GA, Giuffrida D, Milazzo G, Lupo L, *et al.* Cancer risk in patients with cold thyroid nodules: relevance of iodine intake, sex, age, and multinodularity. Am J Med 1992;93:363–9. [Medline] [CrossRef]
20. Gupta A, Ly S, Castroneves LA, Frates MC, Benson CB, Feldman HA, *et al.* A standardized assessment of thyroid nodules in children confirms higher cancer prevalence than in adults. J Clin Endocrinol Metab 2013;98:3238–45. [Medline] [CrossRef]
21. Nikiforova MN, Lynch RA, Biddinger PW, Alexander EK, Dorn GW 2nd, Tallini G, *et al.* RAS point mutations and PAX8-PPAR gamma rearrangement in thyroid tumors: evidence for distinct molecular pathways in thyroid follicular carcinoma. J Clin Endocrinol Metab 2003;88:2318–26. [Medline] [CrossRef]
22. Miyamoto Y, Fukunari N, Omoto K, Kameyama K, Kitaoka M, Kobayashi K, *et al.* Draft of ultrasound diagnostic criteria for thyroid nodule (mass). Jpn J Med Ultrasonics 2011;38:29–30.

Original Paper

Neonatology

Neonatology 2014;105:79–84
DOI: 10.1159/000355818

Received: July 17, 2013
Accepted after revision: September 13, 2013
Published online: November 28, 2013

Survival and Neurodevelopmental Outcome of Preterm Infants Born at 22–24 Weeks of Gestational Age

Masayuki Ochiai[a, c] Tadamune Kinjo[a, c] Yasushi Takahata[a] Mariko Iwayama[a] Takeru Abe[b] Kenji Ihara[a, c] Shouichi Ohga[c, f] Kotaro Fukushima[a, d] Kiyoko Kato[a, d] Tomoaki Taguchi[a, e] Toshiro Hara[a, c]

[a]Comprehensive Maternity and Perinatal Care Center and [b]Medical Information Center, Kyushu University Hospital, Departments of [c]Pediatrics, [d]Obstetrics and Gynecology, [e]Pediatric Surgery and [f]Perinatal and Pediatric Medicine, Graduate School of Medical Sciences, Kyushu University, Fukuoka, Japan

Key Words
Extremely premature infants · Extremely low birthweight · Mortality · Morbidity · Antenatal steroid

Abstract
Background: The limits of viability in extremely premature infants are challenging for any neonatologists in developed countries. The neurological development and growth of extremely preterm infants have come to be the emerging issue following the management in the neonatal intensive care unit. Objective: To assess potential associations between changes in practice and survival/neurodevelopmental outcome, and clinical outcomes of extremely preterm infants born at the limit of viability studied in a tertiary center. Study Design: A retrospective study enrolled 51 infants who had no congenital disorders, and were born at 22–24 weeks of gestational age (GA) in 2000–2009 in our institution. Clinical variables and interventions were studied with regard to one-year survival and developmental quotient (DQ) at 3 years of age. Results: The one-year survival rate of 24 preterm infants born in 2005–2009 (79%) was higher than that of the 27 infants born in 2000–2004 (52%, p = 0.04). Infants born after 2005 underwent less tocolysis (54 vs. 94%, p < 0.01) and more frequently antenatal steroid therapy (32 vs. 6%, p = 0.01) than those born before 2004. The post-2005 survivors (n = 19) received more frequently indomethacin therapy (89 vs. 50%, p = 0.03) and early parenteral nutrition (95 vs. 36%, p < 0.01) than the pre-2004 survivors (n = 14). There were no differences in the proportion of infants who attained a DQ of >50 at 3 years of age between pre-2004 (9/13, 69%) and post-2005 groups (10/17, 59%). Multivariate analysis indicated that extremely premature birth at GA <24 weeks was the sole critical factor for a DQ of >50 in survivors. Conclusions: The perinatal care after 2005 improved the overall survival rate, but not the neurological outcome of preterm survivors at the limit of viability. Neurodevelopmental impairments were associated with extremely premature birth at GA <24 weeks.

Introduction

Recent progress in the perinatal and neonatal care has greatly improved the prognosis of critically ill or premature newborn infants. The limits of viability in extremely premature infants are challenging for any neonatologist

KARGER

E-Mail karger@karger.com
www.karger.com/neo

1661–7800/14/1052–0079$39.50/0

Masayuki Ochiai, MD, PhD
Department of Pediatrics, Graduate School of Medical Sciences
Kyushu University 3-1-1 Maidashi, Higashi-ku
Fukuoka 812-8582 (Japan)
E-Mail ochimasa@pediatr.med.kyushu-u.ac.jp

in developed countries [1–4]. Between 2004 and 2007, the one-year survival rate of infants born at 22–26 weeks of gestational age (GA) in Sweden attained 70%, ranging from 9.8% at GA 22 to 85% at GA 26 weeks [5]. In 2005, the survival rates of Japanese infants during their stay in a neonatal intensive care unit (NICU) were 34.0, 54.2 and 76.6% in infants born at GA 22, 23, and 24 weeks, respectively [6]. On the other hand, the post-NICU neurological development and growth of extremely preterm infants have come to be the emerging issue.

Antenatal steroid therapy was reportedly associated with a significant decrease in the mortality of preterm infants born at GA 22–23 weeks [7]. This intervention was actively introduced in our tertiary center after 2005 for women at high risk of preterm delivery after GA 22 weeks. The alive-born premature infants are at high-risk for a constellation of life-threatening events including cerebral bleeding and sepsis. A small number of survivors at the limit of viability still have an increased risk of physiological and neurodevelopmental problems requiring long-term medical support and socioeconomical services. To assess potential associations between changes in practice and survival/neurodevelopmental outcome, we performed the present study in all infants born at GA 22–24 weeks and treated at a single tertiary center from 2000 to 2009. The favorable limits of viability and neurodevelopmental outcome are discussed with special reference to the prenatal and postnatal management.

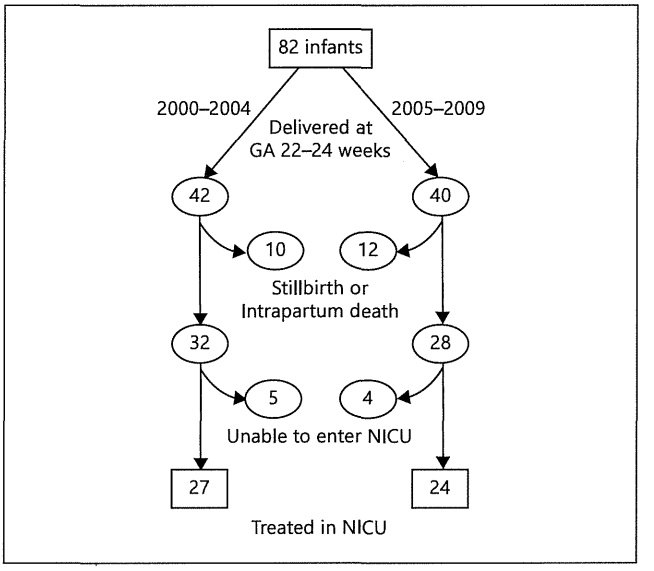

Fig. 1. Demographic characteristics of infants born at 22–24 weeks of GA delivered in 2000–2009 in our single institution. During the 10-year study period, 82 infants were delivered at GA 22–24 weeks, including 42 in 2000–2004 and 40 in 2005–2009. Of the 42 and 40 infants, 10 and 12 were stillbirths or intrapartum deaths, and the 32 and 28 were delivered as live-born infants. Of the 32 and 28 live-born infants, 5 and 4 were unable to enter the NICU because of severe asphyxia or extreme prematurity, and 27 and 24 were treated in the NICU.

Materials and Methods

Study Subjects

The study population included all infants delivered at GA 22–24 weeks at the Kyushu University Hospital in Japan from January 1st 2000 to December 31st 2009 (fig. 1). The maternal and neonatal records of all infants were studied retrospectively. The information collected included previous obstetric history, the present pregnancy and delivery, infant morbidity, treatment, survival, and neurodevelopmental outcome up to 3 years of age. A total of 51 alive infants, all free from congenital diseases, reached the NICU for intensive treatment.

Perinatal period was defined as comprising late pregnancy from GA 22 weeks until birth, labor and delivery, and the first week of life in accordance with the recommendations of the World Health Organization (WHO). Live birth and perinatal mortality were also defined by the WHO recommendations (http://www.who.int/whr/2005/en/index.html). Perinatal mortality included stillbirths and early neonatal deaths. Stillbirth was defined as fetal death before onset of labor. Intrapartum death was defined as stillbirth when the fetus was alive at the start of labor. Early neonatal death refers to a death of a live-born infant within the first 7 days of life, while death covers the remaining period up to the first year of life. GA was determined as the best obstetric estimate based on the last menstrual period, standard obstetric parameters, and ultrasonographic findings. Iatrogenic delivery represented a delivery medically or surgically induced due to maternal and/or fetal indications [8]. Antenatal steroid therapy was defined as the administration of any corticosteroid to the mother between GA 22 and 34 weeks for accelerating fetal lung maturation [9]. Surfactant administration included at least 1 dose of surfactant. Indomethacin treatment was conducted for closure of a patent ductus arteriosus (PDA) diagnosed critically or by echocardiography. Infants with body weight below the 10 percentile of the mean of the Japanese birth size standard data were classified as small for GA (SGA) [10].

Follow-up evaluations, including interval health history, neurologic evaluations, and developmental assessments (developmental quotient, DQ), were performed at 3 years of age. Developmental testing was performed using the Kyoto Scale of Psychological Development 2001 (KSPD) by trained testers. KSPD is a Japanese standard developmental test and is used to assess disabled children by most of public health centers [11]. It is an individualized face-to-face test administered by experienced psychologists to assess child's development in the following three areas: postural-motor (fine and gross motor functions); cognitive-adaptive (non-verbal reasoning or visuospatial perceptions assessed using materials such as blocks, miniature cars, and marbles), and language-social (interpersonal relationship, socializations and verbal abilities). DQ was calculated by dividing the developmental age by chronological